

BRNO UNIVERSITY OF TECHNOLOGY

Faculty of Electrical Engineering
and Communication

MASTER'S THESIS

Brno, 2023

Bc. Jan Sýkora



BRNO UNIVERSITY OF TECHNOLOGY

VYSOKÉ UČENÍ TECHNICKÉ V BRNĚ

FACULTY OF ELECTRICAL ENGINEERING AND COMMUNICATION

FAKULTA ELEKTROTECHNIKY
A KOMUNIKAČNÍCH TECHNOLOGIÍ

DEPARTMENT OF RADIO ELECTRONICS

ÚSTAV RADIOELEKTRONIKY

SUPPORTIVE LANDING MODULE FOR SCIENTIFIC STRATOSPHERIC PROBES

POMOCNÝ PŘISTÁVACÍ MODUL PRO VĚDECKÉ STRATOSFÉRICKÉ SONDY

MASTER'S THESIS

DIPLOMOVÁ PRÁCE

AUTHOR

AUTOR PRÁCE

Bc. Jan Sýkora

SUPERVISOR

VEDOUCÍ PRÁCE

Ing. Aleš Povalač, Ph.D.

BRNO 2023

Master's Thesis

Master's study program **Electronics and Communication Technologies**

Department of Radio Electronics

Student: Bc. Jan Sýkora

ID: 195633

**Year of
study:** 2

Academic year: 2022/23

TITLE OF THESIS:

Supportive landing module for scientific stratospheric probes

INSTRUCTION:

Learn about scientific stratospheric probes and how to communicate with them using wireless technology in the 868 MHz band. Considering the conditions in the stratosphere, design a block concept of an auxiliary landing module containing a control microcontroller, pressure switch, communication module, power supply circuits, GPS locator, and secondary parachute. Verify the functionality of the concept using development kits and demonstrate wireless transmission.

Design the circuit diagram of the system. Design and implement the communication with a ground station in the 868 MHz band. Develop software for the control microcontroller to adjust the impact site from the data supplied prior to launch and from the actual measured telemetry data to perform a secondary parachute release in the event of an inappropriate impact site. Verify the function of the whole system by experimental tests.

RECOMMENDED LITERATURE:

[1] SEMTECH. AN1200.22, LoRa Modulation Basics: Application note [online]. [cit. 2021-05-18]. Dostupné z: <https://www.semtech.com/products/wireless-rf/lora-core/sx1276>

[2] HEGER, Zbynek, Jan ZITKA, Lukas NEJDL, et al. 3D printed stratospheric probe as a platform for determination of DNA damage based on carbon quantum dots/DNA complex fluorescence increase. Monatshefte für Chemie - Chemical Monthly. 2016, 147(5), 873-880. ISSN 1434-4475. Dostupné z: doi:10.1007/s00706-016-1705-y

**Date of project
specification:** 6.2.2023

**Deadline for
submission:** 22.5.2023

Supervisor: Ing. Aleš Povalač, Ph.D.

doc. Ing. Lucie Hudcová, Ph.D.

Chair of study program board

WARNING:

The author of the Master's Thesis claims that by creating this thesis he/she did not infringe the rights of third persons and the personal and/or property rights of third persons were not subjected to derogatory treatment. The author is fully aware of the legal consequences of an infringement of provisions as per Section 11 and following of Act No 121/2000 Coll. on copyright and rights related to copyright and on amendments to some other laws (the Copyright Act) in the wording of subsequent directives including the possible criminal consequences as resulting from provisions of Part 2, Chapter VI, Article 4 of Criminal Code 40/2009 Coll.

ABSTRACT

This diploma thesis focuses on developing of a supportive landing module BUM and its peripherals for the SnHV project. The theoretical part of the thesis presents an overview of the dawn of scientific ballooning till the modern era of ballooning. The second part briefly describes the SnHV project and its parts. The practical part is devoted to designing the BUM, its power supply, developed pressure switch, and its peripherals. The last section describes the experimental testing of the whole developed scientific platform, which was the BUM part of.

KEYWORDS

LORA, Scientific platform, 3D print, HAB

ABSTRAKT

Tato diplomové práce je zaměřena na vývoj podpůrného přistávacího modulu BUM a jeho periferií pro projekt SnHV. Teoretická část práce představuje přehled počátků vědeckého balonového létání až po moderní éru balonového létání. Druhá část stručně popisuje projekt SnHV a jeho části. Praktická část je věnována návrhu BUM, jeho napájení, vyvinutému tlakovému spínači a ostatním periferiím. Poslední část popisuje experimentální testování celé vyvinuté vědecké platformy, jejíž součástí byl BUM.

KLÍČOVÁ SLOVA

LORA, vědecká platforma, 3D tisk

ROZŠÍŘENÝ ABSTRAKT

0.1 Úvod

V dnešním Světě se denně vypustí stovky vědeckých a meteorologických balónů. To je zapříčiněno tím, že tato metoda je relativně levná a výzkumná data a měření z vrstev atmosféry, jsou velmi cená pro výpočetní meteorologické modely, díky nimž můžeme mít relativně přesné předpovědi. v poslední době ale stratosféru objevuje čím dál více univerzit a výzkumných institucí. Ať už je to z výzkumného hlediska, nebo jako otestování svých projektů v prostředí podobnému vesmíru, tedy velmi nízký tlak, velmi nízká teplota, radiace atp.

Každá mise do stratosféry určitě není jednoduchým úkolem, kde je nutné mít multioborový přístup, k řešení problémů, které se vždy při přípráách těchto misí objeví.

Tato diplomová práce byla sepsána v rámci projektu "Společně na hranici vesmíru", jejímž řešitelem byla Hvězdárna Valašské Meziříčí, Ústav chemie a biochemie Mendelovy univerzity, SOSY, Slovenské organizace pro vesmírné aktivity a firmy Spacemanic.

Autor této práce přispěl tomuto projektu návrhem universálního a podpůrného modulu "BUM" a všech jeho periférií. Což je zkratka pro "Bytelný Universální Modul" v anglické verzi "DUM", neboli "Durable Universal Module".

0.2 Řešení

Z prvu bylo nutné si definovat, dle jakých podmínek a pravidel, bude modul navržen. Bylo rozhodnuto, že BUM bude navržen tak, aby byl co nejmenší, nejlehší, co nejvíce spolehlivý a musí odolat podmínkám ve stratosféře. Jako první komponent modulu byla udělána rešerše mikrokontrolerů, které měli vhodné parametry. Nakonec byl vybrán SoC modul ESP32 Wroom32, z důvodu jeho výpočetního výkonu, ceny, bonusových periférií a celkovému poměru ceny/výkonu. Následoval výběr komunikačního modulu.

Pro vědecké mise ve stratosféře není nutný vysoký přenos dat, ve velké míře jsou to pouze poziční koordináty, případně příkazy pro řídicí počítače sond, tedy byla vybrána komunikace LoRa. Následnou rešerší LoRa komunikačních modulů byl vybrán modul RFM95w. Následoval návrh zdroje napájení, kde bylo rozhodnuto, že jako zdroj budou použity dvě NCR průmyslové baterie typu 18650. Z tímto poté byla naržena kaskáda snižujících měničů napětí na 5 voltů a 3.3 voltů.

Následujícím krokem bylo navržení všech periferií, jako indikační ledky, bzučák, vypouštěcí mechanismus sekundárního padáku, který pracuje na principu přepálení vlastce, který drží skložený padáček na vršku sondy. Další zajímavou periferií bylo navržení experimentálního tlakového spínače, který obsahoval v sobě malý balónek, který byl zalepen a uchován v krytu 3D vytištěného krytu, kde v určité vzdálenosti od balónku byl mikrospínač, který se sepnul se vzrůstající výškou, kdy se balónek začal rozpínat. Experimentálním testováním byla zjištěna závislost vzdáleností mezi jazýčkem mikrospínače a balónku, tedy je nyní možné tento tlakový spínač využít k sepnutí sondy v určité výšce, dle potřeby. Celkově byly vyvinuty 3 revize modulu BUM, kdy první byla pouze testovací, na ověření funkčnosti navržených schémat a komunikace mezi mikrokontrolerem a komunikačním modulem RFM95w. Tento krok se vydařil. Následovali dvě nové revize, kdy každá přidávala další funkce oproti svému předchůci. BUM revize 2 přidala sensor teploty a USB převodník. REvize 3 přidala slot na micro SD kartu, komunikaci I2C, změnila se napěťová kaskáda a přidalo se nabíjení baterií. BUM byl navržen jako universální a podpůrný modul pro vědecké mise do stratosféry. Bohužel nebyl zatím plně využit jeho potenciál v podobě přesňování pozice dopadu, protože se vždy zúčastnil misí do stratosféry jako doplnění do plně povolené váhy sondy, a také z důvodu ochrany dražších nákladů, které by mohl špatným výpočtem a nevhodným vyhozením padáku ohrozit.

0.3 Testovací lety

Celkem byly BUM desky ve stratosféře třikrát. První dva lety absolvoval BUM revize druhé, a jeden let BUM revize třetí. Při prvním letu byl chybně nastaven dynamický mód GPS modulu, kdy při výšce nad 12 kilometrů již neodesílal aktuální hodnotu výšky. Tomu se předešlo před druhým startem, naneštěstí při něm došlo nejspíše při startu k částečnému odpojení GPS kabeláže, která poté nekomunikovala. Opět začala komunikovat až v půlce zpětného pádu.

0.4 Závěr

Bylo vyvinuty celkem dvě plně funkční desky universálního modulu BUM, revize dva a tři, které byly ověřeny lety do stratosféry. Byly k nim navrženy periferie a ovládací firmware. Desky obstály a ve stratosférických podmínkách pracovali obstojně. Přesňování polohy dopadu bylo otestováno virtuálně pomocí simulace letu s gps koordináty, nicméně bude ještě nutné udělat více experimentálních testů, například s dronem, než bude tato funkce připravena k ostrému stratu do stratosféry.

SÝKORA, Jan. *Supportive landing module for scientific stratospheric probes*. Brno: Brno University of Technology, Faculty of Electrical Engineering and Communication, Department of Radio Electronics, 2023, 91 p. Master's Thesis. Advised by Ing. Aleš Povalač, PhD

Author's Declaration

Author: Bc. Jan Sýkora
Author's ID: 195633
Paper type: Master's Thesis
Academic year: 2022/23
Topic: Supportive landing module for scientific stratospheric probes

I declare that I have written this paper independently, under the guidance of the advisor and using exclusively the technical references and other sources of information cited in the paper and listed in the comprehensive bibliography at the end of the paper.

As the author, I furthermore declare that, with respect to the creation of this paper, I have not infringed any copyright or violated anyone's personal and/or ownership rights. In this context, I am fully aware of the consequences of breaking Regulation § 11 of the Copyright Act No. 121/2000 Coll. of the Czech Republic, as amended, and of any breach of rights related to intellectual property or introduced within amendments to relevant Acts such as the Intellectual Property Act or the Criminal Code, Act No. 40/2009 Coll. of the Czech Republic, Section 2, Head VI, Part 4.

Brno

.....

author's signature*

*The author signs only in the printed version.

ACKNOWLEDGEMENT

I am grateful to Ing. Jan Zítka and Ing. Jan Šílený for their toil and tears and for being my technical advisors during my work on this thesis. I am also grateful to Ing. Aleš Povalač, PhD. for his helpful guidance and perspective approach.

I want to thank my family and close friends for their support and out-of-the-box tips to improve my thesis.

I would also like to thank Libor Lenža from the Observatory of Valašské Meziříčí and everyone at the Department of Chemistry and Biochemistry at Mendel University for the opportunity to work and pursue a diploma thesis close to my heart.

Contents

0.1	Úvod	7
0.2	Řešení	7
0.3	Testovací lety	8
0.4	Závěr	8
Introduction		23
1	Development of High altitude science	25
1.1	Brief History of High altitude balloons	25
1.2	First atmospheric measurements	25
1.3	Modern scientific HABs	26
2	SnHV - Project Overview	31
2.1	Stack-able modular system	31
2.2	SUPERDUM	33
2.3	DUM - brief	34
3	DUM - Durable Universal Module	35
3.1	Introduction	35
3.2	Microcontroller selection	36
3.3	Communication	37
3.4	Communication module selection	37
3.5	Power management	40
3.6	Periphery	43
3.6.1	Visual signaling	43
3.6.2	Acoustic signaling	44
3.6.3	Experimental pressure switch	45
3.6.4	Secondary chute and release mechanism	46
3.7	DUM - revision 1	49
3.8	DUM revision 2	51
3.9	DUM revision 3	51
3.10	DUM - software	52
3.11	DUM - Ground Station	55
4	Flight tests	57
5	Experimental tests	63
Conclusion		67

Bibliography 69

Symbols and abbreviations 73

List of appendices 75

A Schematics 77

 A.1 DUM revision 1 77

 A.2 DUM revision 2 77

 A.3 DUM revision 3 77

 A.4 DUM - firmware flowchart 77

B Electronic Attachment Table of Contents 91

List of Figures

1.1	First manned hydrogen balloon flight	25
1.2	Ionization Chamber of Victor Hess	26
1.3	Atmospheric layers	27
1.4	Zero pressure balloon diagram	29
1.5	Zero-pressure balloon	29
1.6	Super-pressure balloon	29
2.1	Payload polystyrene sphere	32
2.2	Payload polystyrene cylinder	32
2.3	Modular stack system	32
2.4	Cuvette's cartridge	32
2.5	SUPERDUM block diagram	33
2.6	Initial diagram of the DUM	34
3.1	HAB mission communication	38
3.2	Theoretical LoRa link	41
3.3	Batteries comparison	42
3.4	Step down converter cascade	43
3.5	LED switch circuit	44
3.6	Buzzer driving circuit	44
3.7	Experimental pressure switch circuit	45
3.8	Experimental pressure switch 3D model	46
3.9	Experimental pressure switch test	46
3.10	Pressure versus altitude	47
3.11	Altitude versus distance on the switch	48
3.12	Chute release circuit	49
3.13	Chute release mechanism	50
3.14	Extrenal perfboard	50
3.15	DUM revision 1 pcb	51
3.16	Revision 1 and 2 boards comparison	52
3.17	DUM revision 3 board	53
3.18	Rev 3 idle mode	54
3.19	Rev 3 charging mode	54
3.20	Arduino Dragino shield	55
3.21	Yaggi antenna	55
4.1	DUM - flight test 1	57
4.2	DUM - flight test 1, Altitude	58
4.3	DUM - flight test 2	58
4.4	DUM - flight test 2 altitude	59

4.5	DUM - flight test 3, Altitude	59
4.6	DUM - flight test 3, Altitude	60
4.7	DUM version 1 diagram	60
4.8	Received LoRa transmission	61
5.1	Flight predicted by SondeHub	63
5.2	Descending area of a flight	64
5.3	Live virtual test	65
5.4	Hitted dropzone log	65
A.1	DUM version 1 schematic	78
A.2	DUM version 2 schematic (Page 1)	79
A.3	DUM version 2 schematic (Page 2)	80
A.4	DUM version 2 schematic (Page 3)	81
A.5	DUM version 2 schematic (Page 4)	82
A.6	DUM version 3 schematic (Page 1)	83
A.7	DUM version 3 schematic (Page 2)	84
A.8	DUM version 3 schematic (Page 3)	85
A.9	DUM version 3 schematic (Page 4)	86
A.10	DUM version 3 schematic (Page 5)	87
A.11	DUM version 3 schematic (Page 6)	88
A.12	DUM firmware flowchart	89

List of Tables

3.1	Potential MCUs, adapted from the datasheets [15][16][17].	36
3.2	Czechia and Slovakia LoRa regulation	38
3.3	Potential Transceivers, adapted from the datasheets [18][19][20].	38
3.4	The comparison of the battery properties[23] [24] [25].	42
3.5	The power consumption of the modules [15][18][26].	42
3.6	Physical properties of each revision.	52
3.7	Added functionality per revision.	53

Listings

3.1	Drop zone structure	55
-----	-------------------------------	----

Introduction

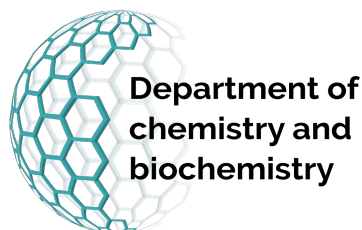
Releasing a stratospheric science probe or HAB (High Altitude Balloon) science probe is a widely known and relatively inexpensive method to test and evaluate various kinds of experiments in conditions similar to space. Many universities and hobbyists around the world release their respective projects with various kinds of experiments every day.

The successful design and deployment of such a probe is a complex problem that requires an interdisciplinary approach. Every project of the scientific stratospheric probe could be divided into two main parts: science and technology. The science part describes the aim of the project and the science behind it. Whilst the technology part describes everything needed to support, carry, etc., for the science experiment.

This thesis aims to design and implementation of a supportive landing module BUM for the primary on-board computer (OBC) called SUPERBUM. BUM and SUPERBUM are part of the SnHV project, which is an abbreviation of "Společně na hranici vesmíru" (together on the border of space), and aims to develop a stratospheric probe platform for scientists and their research in the stratosphere.

The main goal of this project is to develop a stackable platform, similar to the CubeSat platform, that allows individual stack with a custom experiment to be added vertically. The project relies on modern manufacturing processes, including 3D printing.

This thesis was written in cooperation with the Observatory of Valašské Meziříčí, Department of Chemistry and Biochemistry, SOSA – Slovak Organization for Space Activities and SPACEMANIC company.



SPACEMANIC

1 Development of High altitude science

1.1 Brief History of High altitude balloons

Humankind has always been fascinated by the stars and the ability to fly. Through time, many scientists, innovators, and entrepreneurs had many thoughts, and some even tried to invent flying machines of their own. Unfortunately, most of them have failed.

Until the Montgolfier brothers successfully launched their first unmanned hot-air balloon in Annonay in June 1783. In November of that year, they conducted the first manned flight. Simultaneously that year, Jacques Charles successfully tested his unmanned gas balloon with a hydrogen buoyancy medium in Paris. He also made the first manned flight of a gas balloon that year, as shown in Figure 1.1.

All these experiments started an incredible and thriving development era, resulting in the first successful Wright brother's airplane and the first human in Space 120 and 178 years later[1].

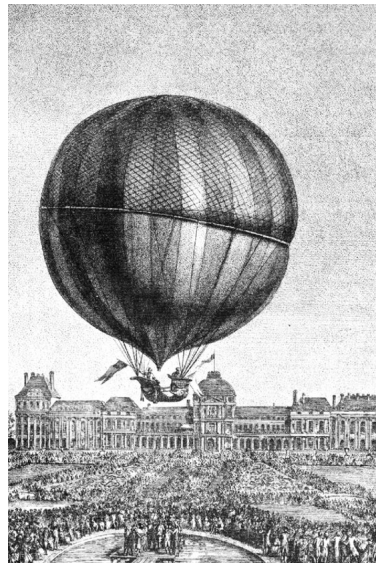


Fig. 1.1: First manned hydrogen balloon flight, adapted from [1].

1.2 First atmospheric measurements

The development of hot-air and gas balloons opened science to the atmosphere. J. Jeffries and J.P. Blanchard were on the first solely scientific flight to study environmental properties in high altitudes in 1784. E. Robertson and M. Lhoest reached

an altitude of 7,000 m in a 5-hour flight from Hamburg to Hannover in 1803. They studied a change in atmospheric radiation in upper altitudes, and an era of the HABs(High Altitude Balloons) flight started. A total of three flights were conducted to determine if magnetic field force decreases or not with an altitude, and they found a decrease in the field's force. In 1804 Joseph L. Gay-Lussac collected air samples from 7,000 m above into an empty bottle of wine and found out the composition of the air was similar to the air at ground level. J. Glaisher was the first to conquer the 10 km altitude mark. These accomplishments led to "balloon mania," which fueled the development and scientific research even more.

Astrophysics fully accepted the use of balloons after observation of the cosmic rays conducted by V.F. Hess in 1912. He carried a simple ion chamber, shown in figure 1.2, up to the altitude of 5,000 m and measured the variation of cosmic rays. He was later awarded the Nobel Prize in 1936 [1] [2].



Fig. 1.2: Ionization Chamber of Victor Hess, adapted from [3].

Unfortunately, all of these remarkable scientists had to endure severe hypoxia, a severe lack of oxygen at higher altitudes during their flights with an altitude close to the peaks of the highest mountain on the planet.

1.3 Modern scientific HABs

Immense success in flights up to the skies exploring the atmosphere during "balloon mania" between 18th and 20th century was just the beginning because most

of them happened in the troposphere. Earth's atmosphere consists of five layers – troposphere, stratosphere, mesosphere, thermosphere, and Exosphere, as shown in figure 1.3. The troposphere stretches up to 15 kilometers from the surface. It contains approximately 75–80 percent of the atmospheric mass (water vapor, dust particles, etc.), and also the majority of clouds form there. The thermal gradient in the troposphere decreases with altitude.

The stratosphere is the next layer, which can extend up to 50 kilometers. The Tropopause is a short gap between the troposphere and the stratosphere. Thermal inversion happens in the intermediate layer, which means that temperature stops declining and starts increasing with altitude. It also denotes the maximum presence of water vapor. From this point on, the atmosphere is arid.

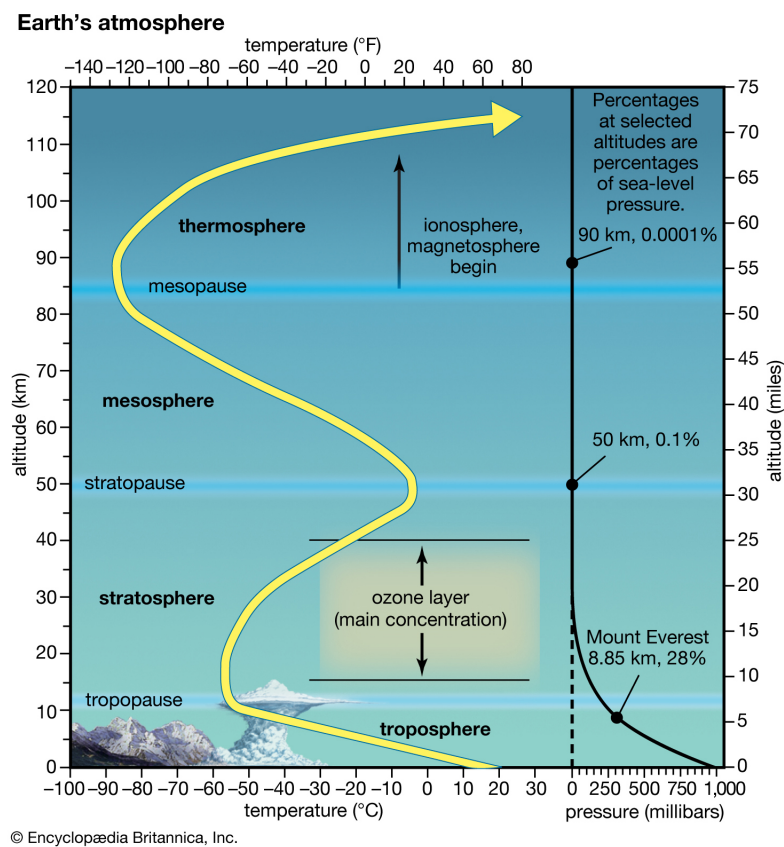


Fig. 1.3: Atmospheric layers, adapted from [4].

The thermal gradient in the stratosphere persists, as does the thermal inversion that began at the Tropopause. As a result of solar heat, the temperature rises with altitude. UV radiation decomposes atmospheric oxygen O_2 into single oxygen atoms, resulting in the formation of ozone O_3 . At the top of the stratosphere, temperatures range from $-55^{\circ}C$ to $0^{\circ}C$

Thermal gradient in the stratosphere continues with thermal inversion started in the Tropopause. That means temperature rises with altitude due to solar heat. The atmospheric oxygen O_2 is decomposed into single oxygen atoms by ultraviolet radiation; thus, attachment of O and O_2 produces ozone O_3 . Temperature ranges from -55°C to 0°C at the top of the stratosphere. The cycle of thermal gradient decreases, and thermal inversion repeats in the mesosphere and the thermosphere. The thermosphere is interesting due to its part abundance of charged ion particles. This ionosphere can be used for radio transmission, reflecting radio waves back to Earth.

Most modern scientific HAB missions use rubber or plastic balloons filled with helium and some kind of OBC(Onboard Computer) to track the location or to support scientific experiments. They are predominantly conducted in the stratosphere, even in the mesosphere. HABs can be divided into these types:

- **ZPB** Zero-Pressure Balloons
- **SPB** Super-Pressure Balloons

The pressure inside ZPB is equal to atmospheric pressure, hence zero pressure. As shown in figure 1.4, it possesses open venting ducts on the bottom, allowing gas to escape and preventing pressurization of the balloon as it rises up. The balloon is partially filled on the ground, and the buoyant gas expands the balloon from the top downwards as it rises. Excess gas is then exhausted through the vents when the balloon is completely expanded and ascend stops. From this point forward, the balloon drifts at a constant altitude. At night buoyant gas cools and shrinks, which causes begin of the descent. It is necessary to drop some ballast weight to maintain the altitude. The gas heats up the next day, but the system is lighter, so the balloon ascends higher and more gas gets exhausted. The cycle repeats until the supply of ballast weight is used, and the balloon goes down. The mission using ZPB usually lasts for several days. The ZPB can lift up to 3,000 kg of payload

In contrast, the SPB maintains a higher internal pressure than the atmospheric pressure. There is no venting duct, and the balloon has to be steadily sealed. The mission, which relies on SPB, can last for a few weeks to a few months with a payload of up to 1,000 kg. The ZPB and SPB are shown in Figure 3.20 and Figure 1.6[5] [6].

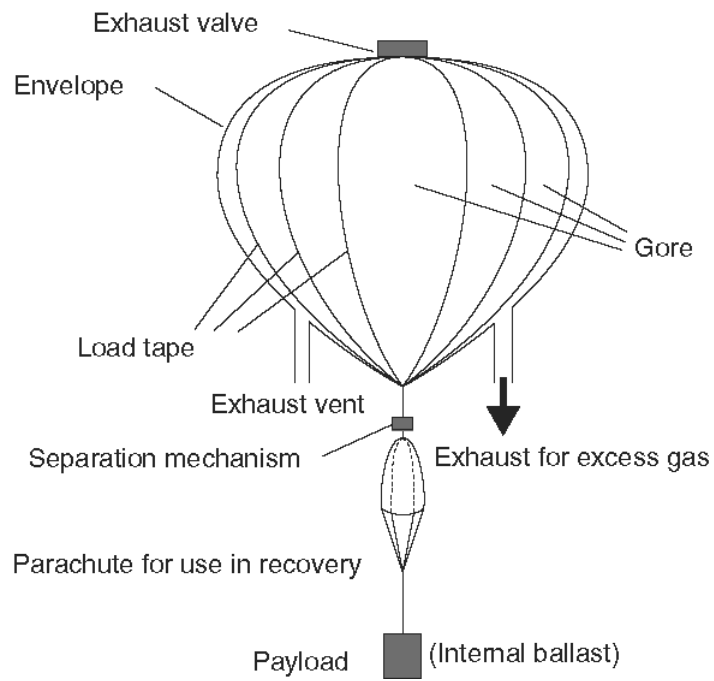


Fig. 1.4: Zero pressure balloon diagram, adapted from [1].



Fig. 1.5: Zero-pressure balloon, adapted from [7].



Fig. 1.6: Super-pressure balloon.

2 SnHV - Project Overview

The SnHV project promoted cooperation and the search for new candidates to work in cross-border development and research-technology teams focused on the development of new equipment, technologies, and innovations. More than two development teams were supported and worked under the guidance of experienced specialists from both the Czech Republic and Slovakia. These teams aimed to jointly develop and construct experimental platforms-modules for research in the stratosphere or in Outer Space.

The project foresaw accurate verification of the developed modules in stratospheric conditions during two test flights. Finally, a joint seminar was held to summarize the project results and further develop cooperation. The SnHV project, throughout its implementation, consisted of these several activities:

- Meetings and professional consultations of the cross-border development teams
- R&D at the sites of the development groups
- Preparation and construction of the prototypes
- Functional and usability testing in laboratory conditions and endurance tests
- Testing in real-life conditions during two stratospheric flights

Expected developed modules from the development groups were:

- Biological experiment module (micro-algae, algae, cyanobacteria)
- Photochemical and particle detection module
- Radio and camera sensing module

2.1 Stack-able modular system

Designing electronics and experiments for stratospheric missions is a challenging process. Key aspects must be secured, such as lightweight, thermal resilience and insulation of components, maintaining a set temperature by heating, battery life, but also complying with the given budget. Many teams around the world use polystyrene as the main body of their probes for its excellent insulation parameters, lightweight and low cost. Two examples are shown in Figure 2.1 and Figure 2.2. The polystyrene cylinder was selected for the SnHV project since SOSA, the Observatory of Valašské Meziříčí, and the Department of Chemistry and Biochemistry had collaborated on a similar project before and had promising experience with this kind of shape. The main idea of the modular system, as shown in Figure 2.3, was to develop a standardized platform or modules for individual experiments and tests. Each experiment would have its own module that can be combined together to make a modular system. All of these modules stacked are held together by two threaded M3 rods. Every

stack is made without the top, which is promptly secured by the bottom of the next module. This way, the whole system is lighter; therefore, a more scientific payload can be used. Since the Department of Chemistry and Biochemistry uses standardized 5ml cuvettes for most of their experiments, every module was developed to hold two 3x6 cuvettes cartridges, as shown in Figure 2.3 and Figure 2.4.

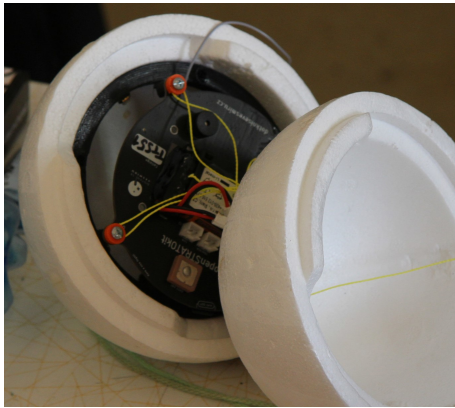


Fig. 2.1: Payload polystyrene sphere.

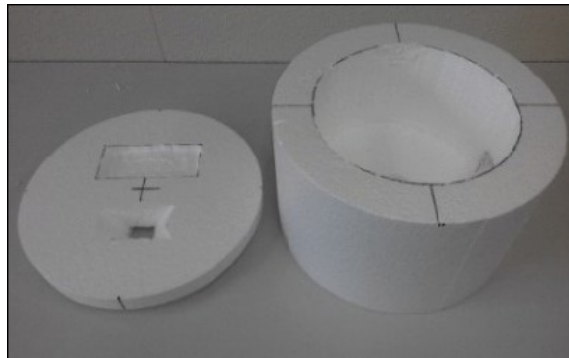


Fig. 2.2: Payload polystyrene cylinder, adapted from [8].

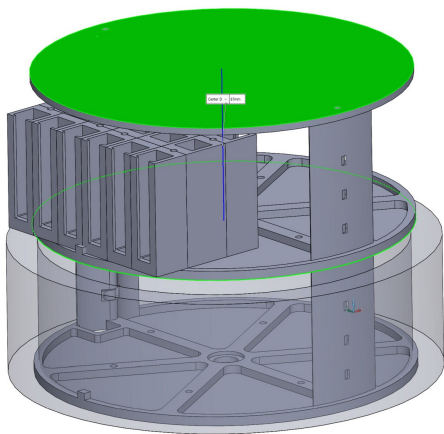


Fig. 2.3: Modular stack system.

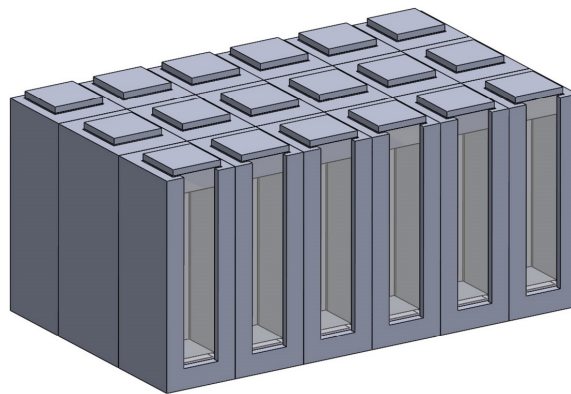


Fig. 2.4: Cuvette's cartridge.

2.2 SUPERDUM

SUPERDUM was the translated English working title of the main OBC during the SnHV project, and the development was done by Ing. Jan Zítka and Ing. Jan Šílený. The primary purpose of the SUPERDUM was to measure the temperatures in all experiments using One Wire temperature sensors, maintain the tempering of the experiments on the set temperature and the data logging. The SUPERDUM also contained the Sun sensor, the UV sensors, the GPS module, the camera module, and the pressure sensor. Tempering the experiments is necessary because the temperature can fall deep below 0°C in the stratosphere, which would surely lead to the destruction of the bio experiments. Logged data can be sent to the GS(Ground Station) through the supportive module DUM. The SUPERDUM and the DUM communicate via UART(Universal Asynchronous Receiver Transmitter). SUPERDUM was developed around OSD335x C-SiP(Complete System in Package) of Octavo Systems. The appropriate features of the OSD335x C-Sip are the minimum operating temperature of -40°C , eight channels ADC(Analog to digital converter), enough storage memory, and affordability. The block diagram of the SUPERDUM is shown in Figure 2.5[9].

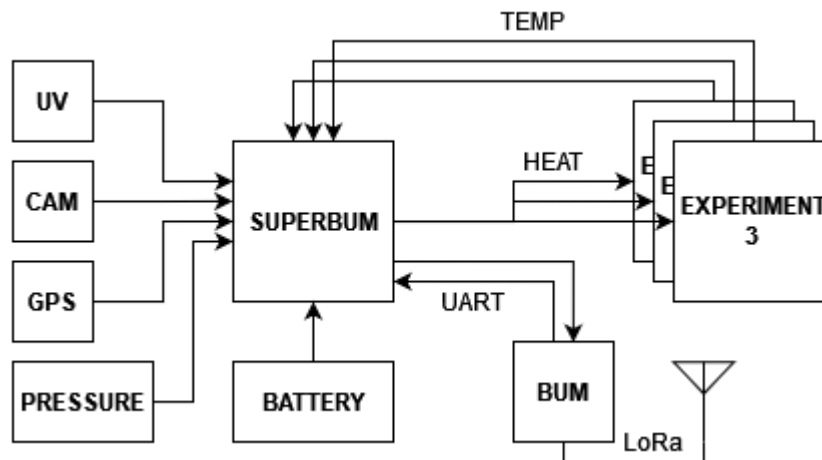


Fig. 2.5: SUPERDUM block diagram.

2.3 DUM - brief

The idea behind DUM (translated English title) in the SnHV project was to be a sort of universal, supportive module like a "live" black box, and if everything goes wrong, and no data are collected at all due to SUPERDUM malfunction, it would help relay the GPS coordinates of the probe to the GS(Ground Station) to secure localization of the probe and at least recover the science experiments, as they are the most valuable part from a research standpoint. A more detailed description of the DUM is in the following chapter 3. The DUM's initial diagram is shown in Figure 2.6

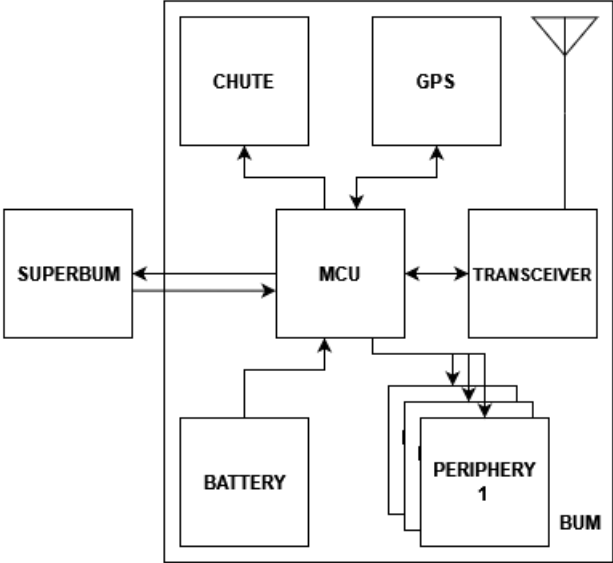


Fig. 2.6: Initial diagram of the DUM.

3 DUM - Durable Universal Module

3.1 Introduction

This diploma thesis covers a subpart of the SnHV project to design a supportive landing module DUM, which was done purely by the author.

As was DUM shortly described in the previous chapter, the intended purpose of the DUM was to be a multi-functional "black box" of the scientific probe. It would allow live communication with the GS, sending telemetry and experiment data back to the ground station to check the functionality of the SUPERDUM and its measurements and tempering. Also, it would allow easier localization after the probe's descent. The DUM was also meant to extrapolate the falling probe's trajectory after the burst of the balloon and compare it with the restricted zones given by the SUPERDUM prior to the start of the mission. If the falling extrapolated trajectory aims to the restricted zone, the DUM should decide if releasing the second chute would help to redirect the trajectory out of the zone, and if so, it shall. The restricted zones are chosen by the operator and can be anything, for example, spacious forests, water reservoirs, villages, or military-restricted zones. All vital parts of DUM are summarized in Figure ??.

The design of the DUM followed these design rules:

- Low Bill of Materials
- Small dimensions to reduce weight
- Must endure low temperature of the stratosphere(-40°C) for the entire flight
- Durability and reliability
- Appropriate price to compute power ratio

In the framework of the SnHV project, a total of 3 DUM revision boards were made. Each iteration added more peripherals and functionality. The development route to the final DUM revision three can be separated into these stages:

- MCU selection
- Communication module selection
- Study ESP32 environment - DUM revision 1
- Planning and design signaling periphery
- Design chute and release system
- Design a pressure switch mechanism
- DUM revision 2
- DUM revision 3

The first revision was meant to be a test unit to what extent the DUM can be done and to test the overall functionality of the design. Subsequently, planning the peripherals was done, such as signaling LEDs, signaling acoustic buzzer, and design of a chute and its release system. A more in-depth description is in the following sections of chapter 3.

3.2 Microcontroller selection

Selecting a suitable MCU (Micro Controller Unit) was done with the said design rules in mind. The MCU shall endure the low temperatures of the stratosphere, have enough computing power, and shall be affordable. Broad research of the MCUs ended with three applicable candidates described in detail in Tab 3.1. The Espressif's ESP32 WROOM 32 SoC was selected due to its outstanding parameters, dual-core, usability, and price of ~4\$ WROOM 32 ready-to-use module with additional features such as Bluetooth and WiFi. Also, many DIY (Do It Yourself) projects are built around the ESP32, and its community creates fabulous things, which was also one of the reasons to choose the ESP32.

Tab. 3.1: Potential MCUs, adapted from the datasheets [15][16][17].

Mfr.	Espressif	STMicroelectronics	NXP Semiconductor
MCU	ESP32	STM32U5	LPC55S2
Core	Xtensa LX6	Cortex-M33	Cortex-M33
No. Cores	2	1	1
F_{clock} [MHz]	240	160	150
ROM [KB]	448	—	—
SRAM [KB]	520	786	256
FLASH	4MB extr.	2MB	512KB
Performace [DMIPS]	~600	240	225
V_{supply} [V]	3V3	3V3	3V3
GPIO	35	14	65
ADC [CHL]	SAR 18/12 bit	SAR 20/14bit, 25/12 bit	5/16 bit
Price [\$]	~4	~15	~10
Temp. tolerance [°C]	-40/+85	-40/+85	-40/+105
Peripherals	UART, SPI, PWM, I2S, GPIO, ADC DAC, TWAI	SAI, I2C, USART, LIN, CAN, SPI, PWM, UART	I2C, I2S, SPI, USART, PWM, USB

3.3 Communication

Communicating with the HAB probe during its mission requires thorough preparation. The communication distances between GS and the probe depend on whether it is a short or long-lasting mission. A short mission lasts for a couple of hours between the start and touchdown of the probe, and the distances are tens of kilometers. Long-lasting missions last for days, and the distances are in the hundreds of kilometers. The probe can even passively fly around the Earth.

Choosing the proper method to communicate with the HAB mission is very important and can depend on the specifics of the mission. Most of the projects use some LPWAN (Low Power Wide Area Network) in the unlicensed ISM (Industrial Scientific and Medical) band. After evaluating the requirements of the SnHV project, the LoRa (Long Range) was selected due to its robustness, reach (up to 100 km), the sufficient data rate for long-distance communication (0.4 kbps around 100km), inexpensive communication modules. LoRa uses 863 MHz–870 MHz in the EU and 902 MHz–928 MHz in the USA. The physical layer is built around Chirp spread-spectrum modulation technology and can use more than one channel. The European channel is mainly 125 kHz, and 125 kHz or 500 kHz for the USA spectrum. The data rate is customizable from 300 bps (bit per second) to 50 kbps (kbit per second). Data rates of the LoRa need to be carefully selected for the trade-off between transmission time and range because LoRa uses a duty cycle and maximum dwell time set by regulation (i.e., the maximum continuous period of channel occupancy by the device). Regulations of LoRa for member states of the SnHV project are shown in Tab 3.4. The project SnHV aimed for a short mission in the stratosphere in one of the project's member countries. The communication module must therefore comply with the country's radio regulations shown in Tab 3.4. The duty cycle, or in other words, the air time, means active transmitting per unit per hour; thus the 1% duty cycle per hour is equal to 36 seconds per hour of active transmission. In order to comply with the regulation, the data transfer is limited to once every 100 seconds[10][11]–[14].

3.4 Communication module selection

The suitable candidates for communication modules are shown in Tab 3.3. The RFM95w was selected as a DUM's transceiver module due to its small size, operating temperature range, and link budget. To ensure a better link budget, the passive five dBi whip antenna shall be used with the communication module used on the flight probe, and the passive ten dBi Yagi antenna shall be used at the GS receiver.

Tab. 3.2: Czech and Slovakia LoRa regulations, adapted from[13][14].

Region	Cz	Sk
Pmax [mW]	25	25
Pmax [dBm]	14	14
Duty cycle [%]	1.0	2.8
$Airtime_{max}/h$ [s]	36	100,8
$Airtime_{max}/d$ [s]	864	2419.2

Tab. 3.3: Potential Transceivers, adapted from the datasheets [18][19][20].

Mfr.	HopeRF	Rf Solutions	Multitech
Module	RFM95w	Lambda62	xDot
Pmax [dBm]	20	22	14
Sensitivity [dBm]	-136	-148	-137
Link budget [dBm]	164	170	147
Data rate [kbps]	up 300	up 300	up 20
Bandwidth [kHz]	125 - 500	7.8 - 500	125 - 500
Spreading Factor	6 - 12	5 - 12	6 - 12
Size [mm]	16X16	23x20	24x24
T range [°C]	-55/+70	-40/+85	-40/+85
Price [\$]	~7	~7	~25

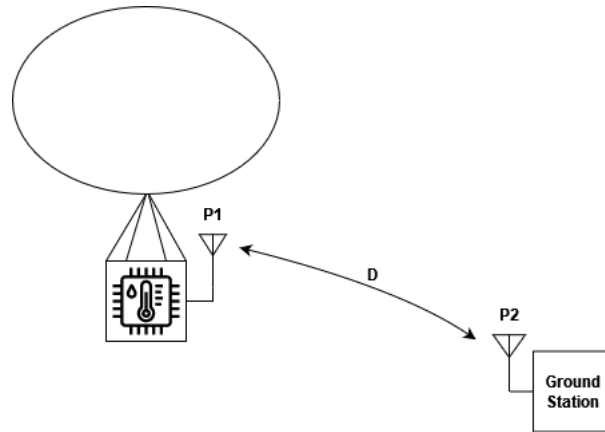


Fig. 3.1: HAB mission communication

With knowledge of the regulations and the communication module properties, estimating the theoretical maximum communication distance is possible. An illus-

tration of the communication between GS and the probe over the distance D is shown in Figure 3.1. It is common to use both suffix notations $(1/t)$ for the transmitter and $(2/r)$ for the receiver. The power received P_2 or P_r at the distance D from the source can be determined by the size of the Poyinting's vector Π_2 ,

$$\Pi_2 = \frac{P_1}{4 \cdot \pi \cdot D^2} \quad (3.1)$$

where P_1 is the input power fed to the antenna and $1/D^2$ represents the attenuation of the signal power between two points due to the spherical spreading over the distance. For the power P_2 is needed to include the gain of the antenna G ,

$$G = \frac{4 \cdot \pi}{\lambda^2} \cdot A_e \quad (3.2)$$

where λ is the wavelength of the transmitted wave and A_e is the effective aperture of the antenna. Then the P_r would be,

$$P_r = \Pi_2 \cdot A_{er} = \frac{G_t \cdot P_t \cdot A_{er}}{4 \cdot \pi \cdot D^2} \quad (3.3)$$

expressing the effective aperture of the receiver A_{er} from the Equation 3.2 and applying it to the Equation 3.3 which would result into Friis transmission equation,

$$P_r = P_t \cdot \frac{G_t \cdot G_r \cdot \lambda^2}{(4 \cdot \pi \cdot D)^2} \quad (3.4)$$

which can be transformed into a convenient dB form,

$$P_r(dBm) = P_t(dBm) + G_t(dB) + G_r(dB) - 20 \cdot \log_{10} \left(\frac{\lambda}{4 \cdot \pi \cdot D} \right) \quad (3.5)$$

$$P_r(dBm) = P_t(dBm) + G_t(dB) + G_r(dB) - FSPL \quad (3.6)$$

where P_r is received signal power, P_t is transmitted power, G_t and G_r are antennas' gain, respectively, FSPL (Free Space Path Loss) and L_M is miscellaneous losses, for instance, impedance mismatch loss, polarity, and cable losses. The FSPL equation expressed from the Equation 3.5 and the Equation 3.6 in dB-form would be,

$$FSPL(dB) = 20 \cdot \log_{10}(D) + 20 \cdot \log_{10}(f) - 147.55 \quad (3.7)$$

where D is the distance and f is the transmitting frequency. Therefore, attenuation of the free space rises with higher frequencies and distances. The Friis transmission equation assumes perfect conditions of the communication link, such as clear LoS(Line of Sight), no multipath scattering, perfect antenna alignment, and ideal

impedance matching. All of these conditions are almost never met in real communication. Fortunately, it is straightforward to add these or other miscellaneous attenuations L_M into Equation 3.6 to get a more accurate result.

$$P_r(dBm) = P_t(dBm) + G_t(dBm) + G_r(dBm) - FSPL(dB) - L_M(dB) \quad (3.8)$$

Applying the minimum sensitivity of the communication module $P_r = -136$ dBm and allowed maximum transmit power $P_t = 14$ dBm into the Equation 3.8 assuming theoretical calculation without antenna's gains would net maximum free space loss of $FSPL_{max} = 147$ dB. Expressing the distance D from the FSPL part in the Equation 3.5 would net,

$$D = \frac{c}{4 \cdot \pi \cdot f \cdot 10^{-\frac{FSPL}{20}}} \doteq 775km \quad (3.9)$$

which is pretty close to the last LoRa communication record of 741km held by Manuel Cuesta with his PaPe I probe, just to be broken again just a few hours later by Enrique Torres and his Diana I probe with (766km). The PaPe I probe used the same receivers as was chosen for the DUM - RFM95w. Detailed relation of FSPL and LoRa signal strength is shown in Figure 3.2[21][22][28].

3.5 Power management

Choosing the right battery for the stratospheric probe is a crucial task since there is a near-spacelike environment, e.g., low or close to zero pressure, radiation, and low temperature. Therefore, the discharge temperature range of the battery should be as wide as possible. Also, maximum weight reduction is one of the top design priorities, and it is necessary to choose the lightest and the energy-densest battery. In Tab 3.4 and in Figure 3.3 are shown the most used battery types. Comparing these properties, the Li-ion NCA battery was chosen for the DUM's main battery, more specifically, the NCR18650GA from Panasonic, due to its overall best Volumetric density and energy density. The only downside is the shorter life cycle of the battery. The power management should cover the entire flight duration(2-3 hours). The maximum power consumption of the DUM and its sub-parts are shown in Table 3.5. It is implausible that DUM would operate on the maximum power for the whole flight, hence air-time restriction; due to low temperature in the stratosphere, the battery's capacity decreases. The minimal battery capacity should be calculated with that in mind [27].

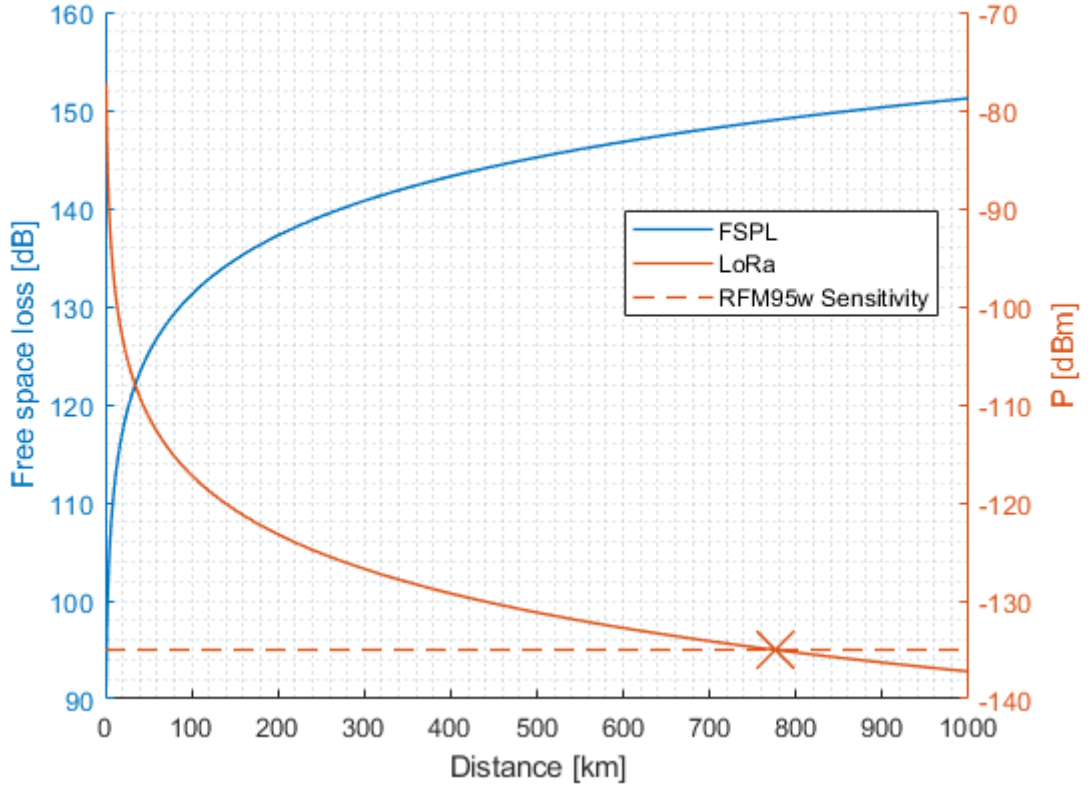


Fig. 3.2: Theoretical LoRa link.

Using the P_{total} from the Tab 3.5 and adding the sufficient engineering safety margin of 15% makes $P_{\text{total}} \doteq 1.5 \text{ W}$. Assuming the whole one hour in maximum power mode, thus power needed is $P = 1.5 \text{ Wh}$, 3.6V 18650 Li-Ion industrial battery to be used, then the capacity needed be determined as,

$$P(\text{Wh}) = C_{\text{min}}(\text{Ah}) \cdot V_{\text{batt}}(\text{V}) \rightarrow C_{\text{min}}(\text{mAh}) = \frac{P}{V_{\text{batt}}} \cdot 1000 \frac{1.5}{3.6} \cdot 1000 \doteq 420 \text{mAh} \quad (3.10)$$

where C_{min} is the minimum battery capacity for one hour in a function mode and V_{batt} nominal voltage of the battery. The chosen NCR battery = $C_{\text{batt}}(\text{mAh}) = 3450$ would net,

$$\text{Batterylife} = \frac{C_{\text{batt}}}{C_{\text{min}}} = \frac{3450}{420} \doteq 8.2 \text{hour}, \quad (3.11)$$

which is more than enough for the short HAB mission because the average power consumption will be much lower than that. Assuming half of the maximum power consumption extends battery life two times. Parallel connection of batteries is not

Tab. 3.4: The comparison of the battery properties[23] [24] [25].

Type	Nickel		Li-ion			
Name	NiCd	NiMH	LFP	LCO	NMC	NCA
Cell chemistry	NiCd	NiMH	LiFePO ₄	LiCoO ₂	LiNiMnCoO ₂	LiNiCoAlO ₂
Energy Density [Wh/kg]	45-80	60-120	90-120	150-200	150-220	200-260
Volumetric Density [Wh/L]	70-220	160-400	333	560	580	600
Life Cycle	1000	300-500	>2000	500-1000	1000-2000	500
Cell Voltage [V]	1.2	1.2	3.3	3.6	3.6	3.6
Discharge Temp. range [°C]	-20/+65	-20/+65	-30/+55	-20/+60	-20/+55	-20/+60

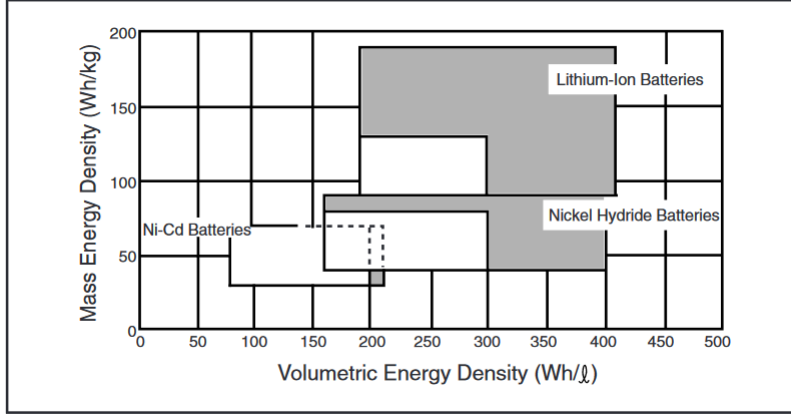


Fig. 3.3: Batteries comparison, adapted from [23].

necessary for most missions. The industrial Li-on 18650 batteries operate approximately from 3 V to 4 V cell voltage.

For the DUM revision one and then also used on revision two, a step-down power regulator cascade was developed as shown in Figure 3.4 and in full schematics in Appendices A.1 and A.2. The cascade consists of two LDOs L4941BDT-TR of STMicroelectronics and NCV8186BMN330TAG of OnSemi to reduce the incoming battery voltage to 5v and 3v3 rails. Each device is capable of supplying current up to 1A. Hence it is required to use two NCR batteries in a series.

Tab. 3.5: The power consumption of the modules [15][18][26].

Module	I _{max} [mA]	V _{supply} [V]	P[W]
ESP32	239	3.3	~0.8
RFM95w	120	3.3	~0.4
NEO6	21	3.3	~0.1
Total	380	3.3	1.3

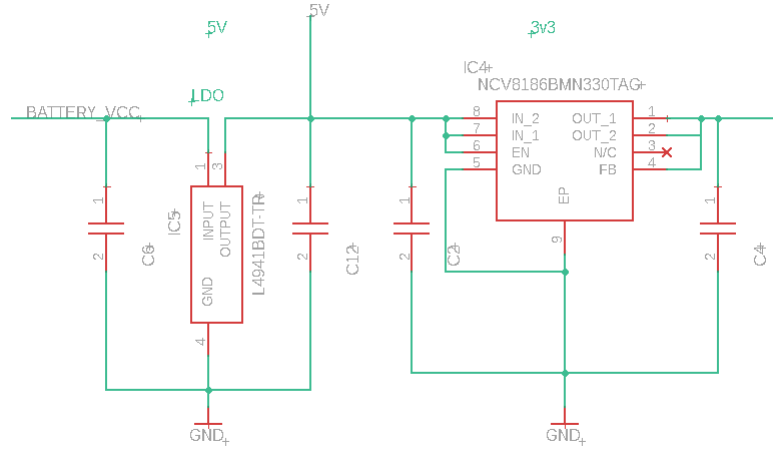


Fig. 3.4: Step down converter cascade.

3.6 Periphery

3.6.1 Visual signaling

The DUM purpose of the easing of localization of descended probe can be done in three ways,

- visually - eyes - signaling LEDs
- acoustically - ears - acoustic buzzer
- radio signal - LoRa

and the DUM is capable of doing it all. For a visual indication of the DUM, the OVLEW1CB9 high-intensity LED was chosen. It has luminous intensity $I = 35000$ mcd at forward current $I_F = 20$ mA, and viewing angle $\Theta = 15^\circ$. To control and drive the LED, the driving circuit was designed as shown in Figure 3.5. The circuit is made from the switching transistors SC4617EBHZGTLR and the current limiting resistors, which were calculated as shown in Equation 3.12,

$$R_c = \frac{V - V_F}{I} \rightarrow \frac{7.2 - 3.2}{20 \cdot 10^{-3}} = 220\Omega, \quad (3.12)$$

where V is the Voltage of the source, V_F is the forward voltage of the LED, and the I is the wanted current. The resistor value was kept for R_c . The base of the transistor is connected to the driving PWM (Pulse Width Modulation) GPIO (General Purpose Input Output) pin of the MCU with base resistor R_b which can be calculated from the nominal voltage of the GPIO pin $V = 3.3V$ and V_{besat} of the transistor shown in Equation 3.13 [29] [34].

$$R = \frac{V - V_{besat}}{I} \rightarrow \frac{3.3 - 1}{1 \cdot 10^{-3}} = 2300\Omega \quad (3.13)$$

The base resistor value was set to the closest row to $R_b = 2400\Omega$.

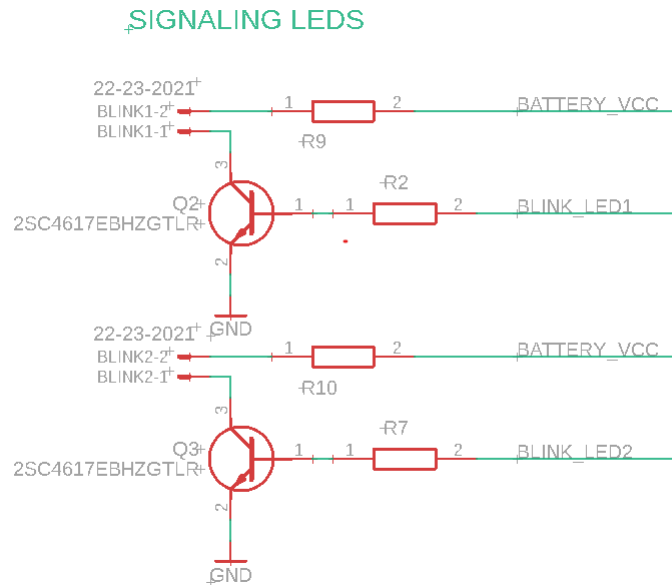


Fig. 3.5: LED switch circuit.

3.6.2 Acoustic signaling

Similarly, as described in the previous subsection 3.6.1, the same switching circuit was used for the buzzer with a rectifier diode added due to the nature of the inductive character of the buzzer. This circuit is made to be used with available DC (Direct current) 5V buzzers.

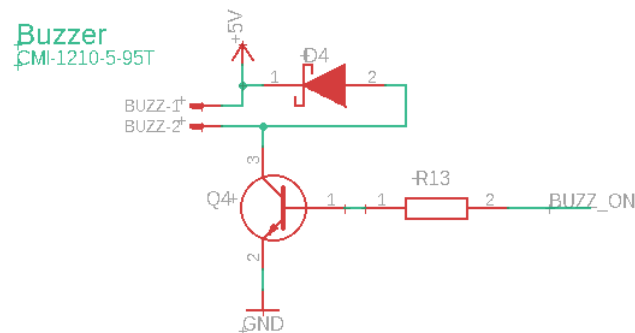


Fig. 3.6: Buzzer driving circuit.

3.6.3 Experimental pressure switch

The idea behind the experimental pressure switch was to try to develop a cheap, customizable "turn on/off" pressure switch from the everyday components. The pressure switch works on the principle of expansion of the sealed kid's water balloon, which begins to expand with increasing altitude until it closes the micro switch. The circuit behind it is, as intended, simple and consists only of just a micro switch and a pull-up resistor. To set the altitude at which the switch triggers on or off is done by adjusting the distance between the switch reed and the small balloon. The circuit and the designed pressure switch are shown in Figure 3.7 and Figure 3.8. As shown in Figure 3.8 there can be seen the switch cover, the running surface for setting the switch distance from the balloon, and a small plastic scientific tube on which the balloon is threaded and glued to prevent any leaks. The scientific tube was used due to its high availability from the scientific team of the SnHV project when the development of the stackable system was done. The 3D model, which is added in Electronic appendices, can be quickly remodeled to fit the balloon, or it might be faster to print the plastic tube.

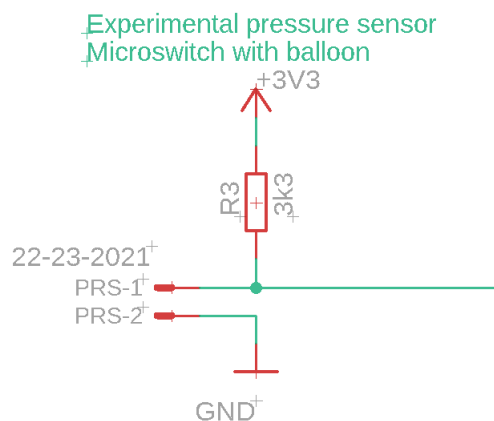


Fig. 3.7: Experimental pressure switch circuit.

As shown in Figure 3.9, a series of tests with the experimental pressure switch was done in the vacuum of a lyophilizer machine to determine the function of the pressure the balloon sets the switch. The function has been detected and is shown in Figure 3.11, the bottom part of the 3d model has spots 5 millimeters apart starting from the 0, meaning zero distance between the balloon and the reed of the switch. Thanks to Figure 3.10 and Figure 3.11, it is possible to set the desired value of the switching altitude to read an appropriate altitude's pressure value and then adjust the distance between the reed and the balloon accordingly.

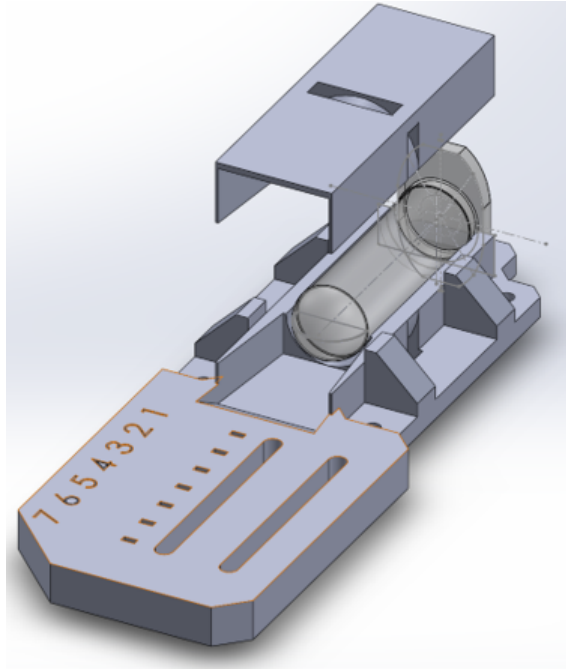


Fig. 3.8: Experimental pressure switch 3D model.

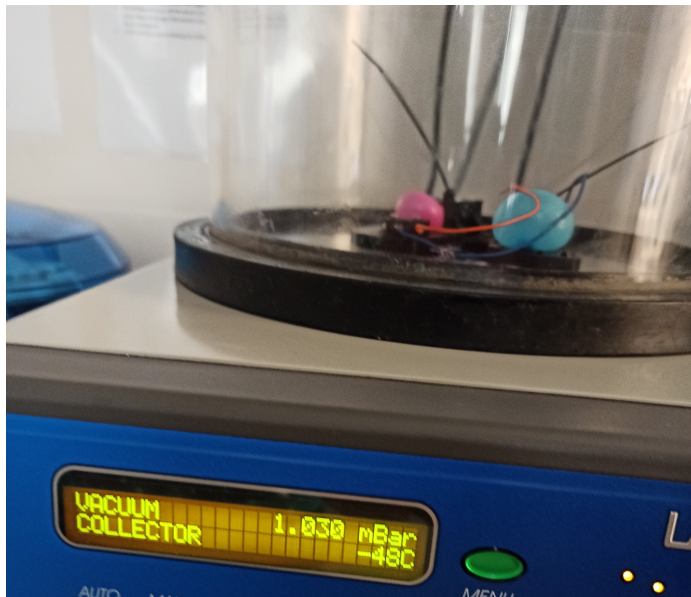


Fig. 3.9: Experimental pressure switch test.

3.6.4 Secondary chute and release mechanism

Designing the release system of the secondary chute needed set requirements such as:

- Reliability

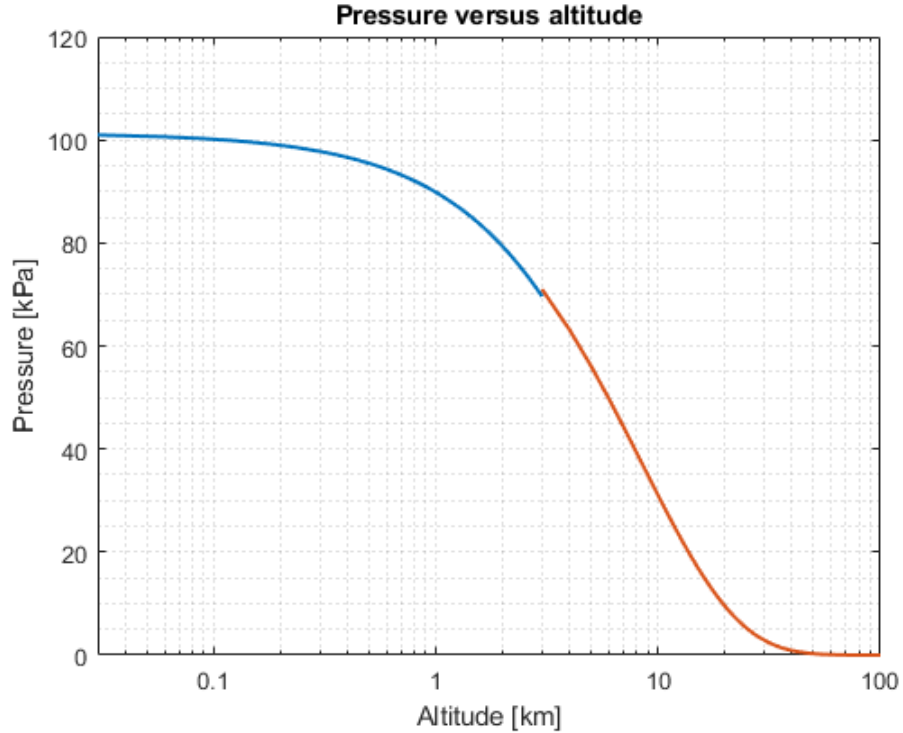


Fig. 3.10: Pressure versus altitude.

- Simplicity

With these requirements in mind, the release mechanism is in the form of attaching the wrapped chute to the top of the probe using a fishing wire. The wire is then melted, and the chute is then opened by the surrounding wind flow. The circuit shown in Figure 3.12 is based on a FZT651QTC high-performance BJT (Bipolar Junction Transistor) performance transistor and the resistive heating wire. Once again, it was necessary to calculate the needed parameters, such as the base resistor and the length of the resistive wire and its current, to reliably melt the fishing wire. The first step that what was taken was obtaining the resistive wire. The ODP-KANO1 from the ELCHEMCO manufacturer was selected. It has a specific resistance of $R = 53.1\Omega/m$, a diameter $d = 0.18mm$, and a maximum working temperature of $T_{max} = 1300^{\circ}C$ and is made from kanthal.

Experimenting with a laboratory power supply, it was found that the minimum current $I_{min} = 0.75A$ at nominal two NCR batteries in series $U = 7.6V$ melting the fishing wire took approximately $t_{min} = 6s$. By further increasing the current to $I = 1.25A$, instantaneous breakage of the wire was guaranteed. Be noted that in Figure 3.12, there is input voltage $V = 12V$, which revision one and revision two

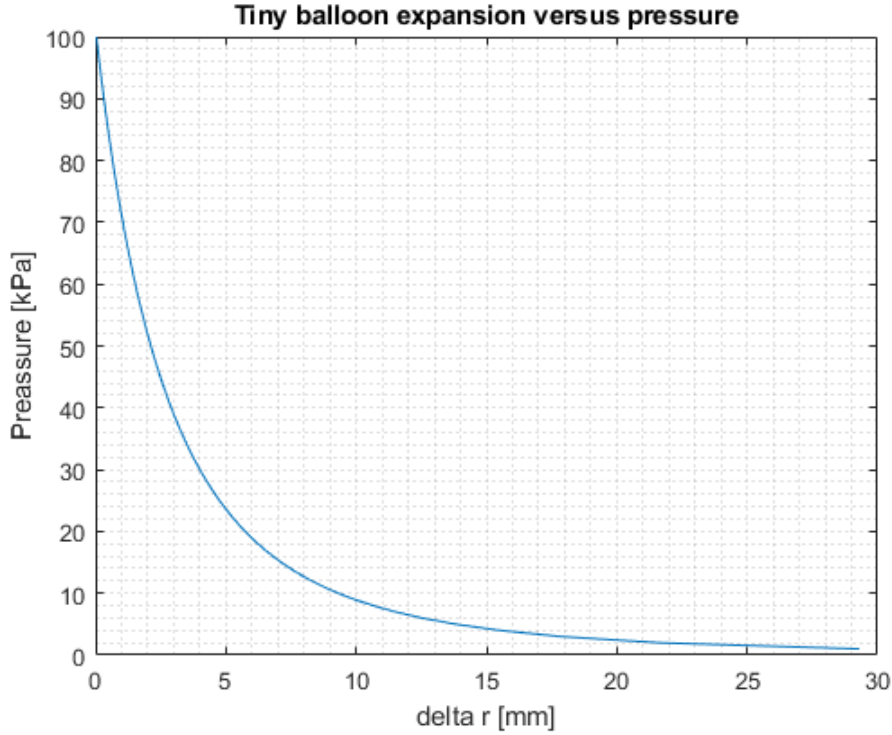


Fig. 3.11: Altitude versus distance on the switch.

does not have. Not that is due to the DUM revision three power cascades changed. A more detailed description is in each separate section of DUM revisions. These calculations were therefore done for the most recent revision 3. With the knowledge of wanted collector current $I_c = 1.25A$ the calculation is then shown in Equation 3.14.

$$R_c = \frac{V_{supply} - V_{cesat}}{I_c} = \frac{12 - 0.12}{1.25} \doteq 9.5\Omega \quad (3.14)$$

With known R_c , the I_b current needed to set R_b can be calculated from Equation 3.15.

$$I_c = h_{fe} \cdot I_b \rightarrow I_b = \frac{I_c}{h_{fe}} = \frac{1.25}{170} \doteq 7.5mA \quad (3.15)$$

With known I_b the needed resistor R_b can be calculated from Equation 3.16.

$$R_b = \frac{V_{gpio} - V_{besat}}{I_b} = \frac{3.3 - 0.9}{7.5 \cdot 10^{-3}} \doteq 326\Omega \quad (3.16)$$

R_b fits nicely to the E12 resistor row, but the R_b was lowered to $R_b = 270\Omega$ because it was available in the author's inventory. With the back computing with a new R_b , $I_b \doteq 9mA$, $I_c = 1.5A$ and $R_c \doteq 8\Omega$.

It is also important to compute the power dissipation shown in Equation 3.17.

$$Pt = U_{besat} \cdot Ib + U_{be} \cdot Ic = 0.9 \cdot 9 \cdot 10^{-3} + 0.12 \cdot 1.5 = 0.1881W \quad (3.17)$$

transistor thermal power dissipation is $Pd = 2W$, and thermal junction to ambient resistance is $R_{\theta JA} = 12.9^{\circ}C/W$. With these parameters, the transistor's temperature can be calculated in Equation 3.18.

$$T = T_A + R_{\theta JA} \cdot Pt = 25 + 12.9 \cdot 0.1881 \doteq 37^{\circ}C \quad (3.18)$$

The temperature rise of 12° above ambient temperature is negligible. One last calculation is needed, and it is the length of the resistive wire. Its length is obtained from its said specific resistance $R = 53.1\Omega/m$ and use of a rule of proportion, the length is $l = 15cm$. The resistive heating wire was mounted externally due to the mobility of the mounting inside of the probe. The wire was stretched over pins on the perf board and then secured in the position by the jumpers as shown in Figure 3.14 [35].

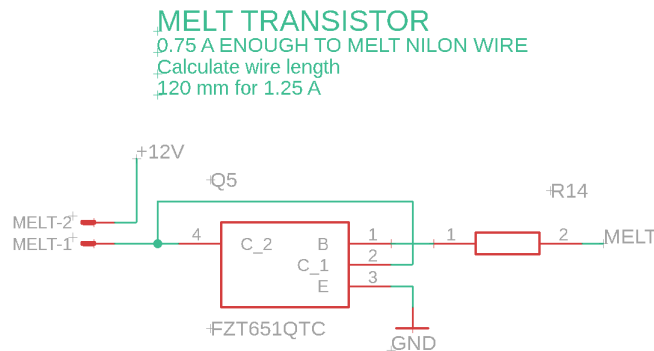


Fig. 3.12: Chute release circuit.

3.7 DUM - revision 1

With the MCU, communication module and power source picked and designed, the DUM revision one, as shown in Figure 3.15 was created in the EAGLE software from AUTOCAD and sent for manufacturing. As can be seen in the left right-corner, there has been a mistake in the board design in which the polygons' priorities were mismatched, and one power source polygon was shorted to the ground and needed a correction with a screwdriver. Apart from this error, the board was functional and passed the goal of verification of the designed power cascade, ESP32, and RFM95w communication with each other and over LoRa.



Fig. 3.13: Chute release mechanism.

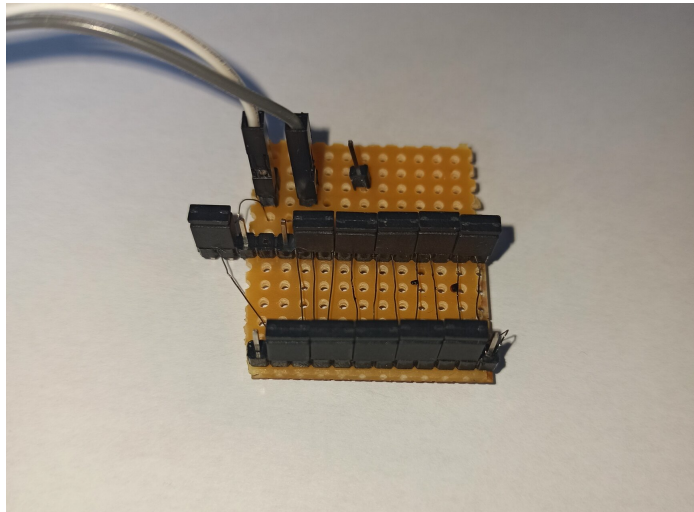


Fig. 3.14: External perfboard.



Fig. 3.15: DUM revision 1 pcb.

3.8 DUM revision 2

The second iteration of DUM was much more integrated than the previous one, adding a temperature measurement via OneWire communication using a DS18B20+ temperature sensor from Analog Devices. Also, the USB communication was added because revision 1 was still only programmable over the USB bridge. The board area was reduced by 44% and the weight by 72 grams as shown on Tab 3.6. The revision one and revision two side by side are shown in Figure 3.16.

3.9 DUM revision 3

In revision three, the power supply cascade has changed compared to previous revisions to include a boost converter that firstly raises the battery supply voltage to 12V, and then the cascade is the same 5V and 3.3V. It is no longer necessary to have two batteries in series as the power source and have only one battery, thus reducing weight, or if necessary, it is possible to connect the batteries in parallel to increase capacity. The boost converter's schematic is shown in Appendix A.11. The size and weight of the revision three board has increased compared to the previous one, but the weight-to-area ratio is almost halved. Also, more features were added, such as +12V power supply, Micro SD card, I2C communication, and battery charging via

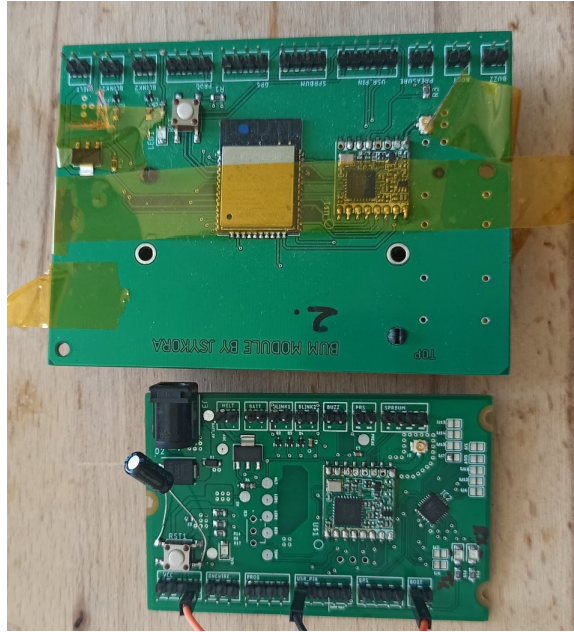


Fig. 3.16: Revision 1 and 2 boards comparison.

Tab. 3.6: Physical properties of each revision.

	Length [mm]	Width [mm]	Area [dm ²]	Weight [g]	Battery [g]	Total weight [g]	Weight/Area [g/dm ²]
Rev 1	100	68.5	68.5	88	100	188	2.745
Rev 2	77	50	38.5	16	100	116	3.01
Rev 3	100	60	60	48	50	98	1.633

USB, and the RFM95w's antenna connector was changed from U.FL to SMA. All changes are clearly shown in Tab 3.7. In Figure 3.17 is shown the latest revision 3 of the DUM. In the Figure 3.21 is shown the thermal characteristics of the idle and charging mode of the battery. The view is taken from the bottom side, where all power converters and battery management chips are located. The online design tool Webench from Texas Instruments was used to design the boost converter circuit [30].

3.10 DUM - software

The DUM, upon attaching the power supply, shall check if it has stored dropzones inside the SPIFFS Filesystem. Then the series of initializations of the peripherals shall be done. The first initialization of them is the GPS. It disables the NMEA messages, changes the baud rate to 115200 Bd, frequency rate to 10 Hz, disables

Tab. 3.7: Added functionality per revision.

	Functionality added
Rev 1	-
Rev 2	OneWire, USB bridge
Rev 3	+12V, Micro SD, I2C, Battery charging

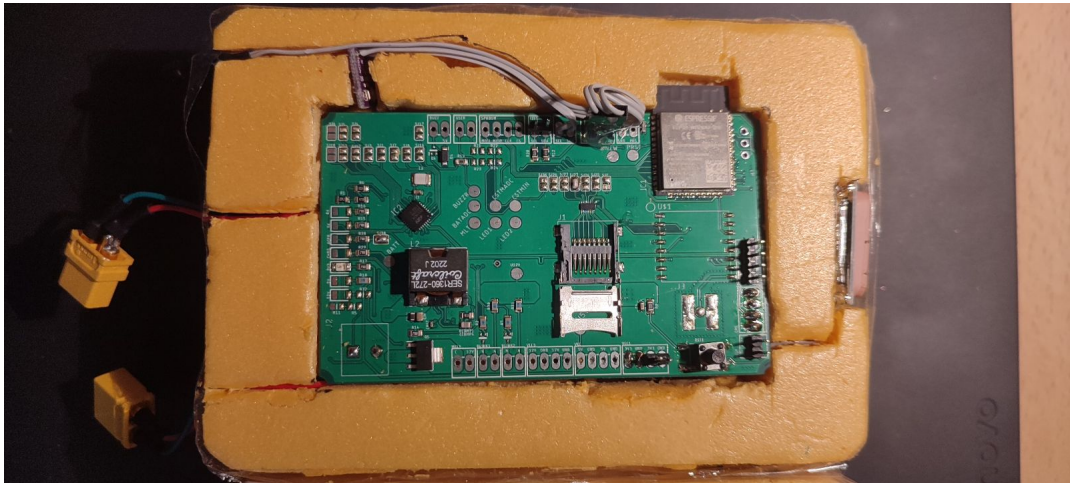


Fig. 3.17: DUM revision 3 board.

all necessary channels except the GPS, enables NEO8M NAV-PVT messages, and sets the dynamic mode to airborne 2g. After that, the ADC, Temperature, and I2C peripherals are initialized. Lastly, initialization is done by the SD card'S firmware because it is the most important one. If the Micro SD card is not present, firmware shall then perform a series of indication signals via LEDs and buzzer and then restart the program. This is a safety precaution to prevent badly inserted or faulty Micro SD card, because data is the most valuable part of the mission. The Core 0 shall start to service the main loop function. The second core is in idle mode till it gets a flag for GPS fixes buffer is filled, then it performs a test, if the trajectory is heading to any of the stored drop zones. That is done by calculating the polynomial trajectory coefficient from the stored GPS fixes buffer by using the arduinoCurveFitting library. The library uses the least square regression. The DUM prepares the two

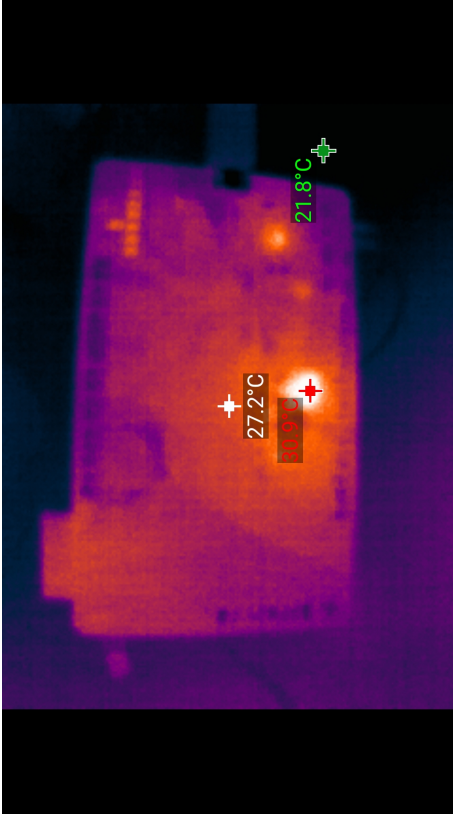


Fig. 3.18: Rev 3 idle mode.

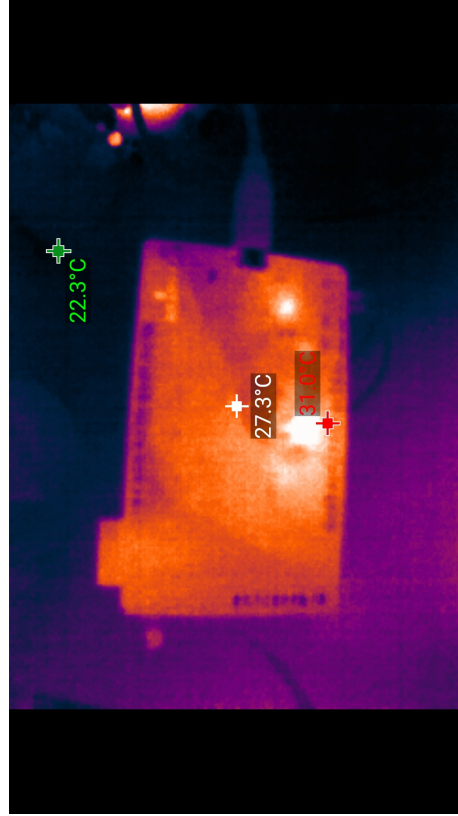


Fig. 3.19: Rev 3 charging mode.

sets of coefficients, altitude versus longitude and altitude versus latitude, for the two polynomial equations of the N-th order. For the testing, the second and third order was used. Upon successful computing of the polynomial coefficients, the polynomial equations are prepared and then executed. With the results of two sets of fitting, the 3D trajectory is made. The DUM then computes the distance on the surface of the sphere between computed coordinates and all the stored drop zones coordinates. If the distance is lower than the dropzone's radius, then the drop zone was hit, and the function `hitTest()` returns a true flag. The DUM then runs the `hitTest` once more with the secondary chute deceleration coefficient. If the `hitTest` then returns false, it means the trajectory ends up outside the dropzone and shall release the secondary chute. If it returns true, it means the dropzone will be hit no matter the secondary chute and shall do nothing. Stored dropzone's parameters are shown in Listing 3.1. In the meantime of filling the gps fix buffer, the Core 0 services LoRa handle to send packets to the ground station, check the pressure switch and call `datalog`. A flowchart of the DUM's firmware is attached in Appendix A.12[31].

Listing 3.1: Drop zone structure

```
1 //dangerous drop zone information
2 //4B float/4B float/4B float/4B float
3 typedef struct DropZone_t {
4     float latitude;
5     float longitude;
6     float altitude;
7     float radius; //we will use meters
8 };
```

3.11 DUM - Ground Station

The Dragino shield for the Arduino Uno with the passive Yagi antenna was used as the ground station. It uses the same LoRa transceiver RFM95w as the DUM. With the DUM revision three it is possible to use with as the ground station as well [31].

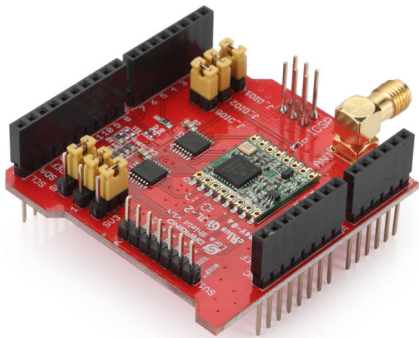


Fig. 3.20: Arduino Dragino shield, adapted from [31].



Fig. 3.21: Yaggi antenna.

4 Flight tests

The DUM has successfully survived three stratospheric flights in total. The second revision has endured two flights and. one flight for the revision three. On the first flight the error was made by not setting the dynamic mode of the GPS to airborne 2g; thus the altitude was cut off, as shown in Figure 4.2, which was resolved before the next flight. Unfortunately, in the second flight, the GPS module probably got partially disconnected, as shown in Figure 4.4, and started working again in mid-fall, where the descend shaking might get it connected back. On the third flight, everything seemed to work successfully, and the data is shown in Figure 4.5 and Figure 4.6. During the first two stratospheric flights the testing of LoRa communication was conducted. There was a steady communication link between GS and the probe for a total distance of 11.4 km, as shown in Figure 4.7 and an example of data packets received is shown in Figure 4.8. So far, the DUM was not tested in the full configuration because in all flights missions it has filled up the unused mass of the probe. Another reason was not to endanger the expensive payload onboard.

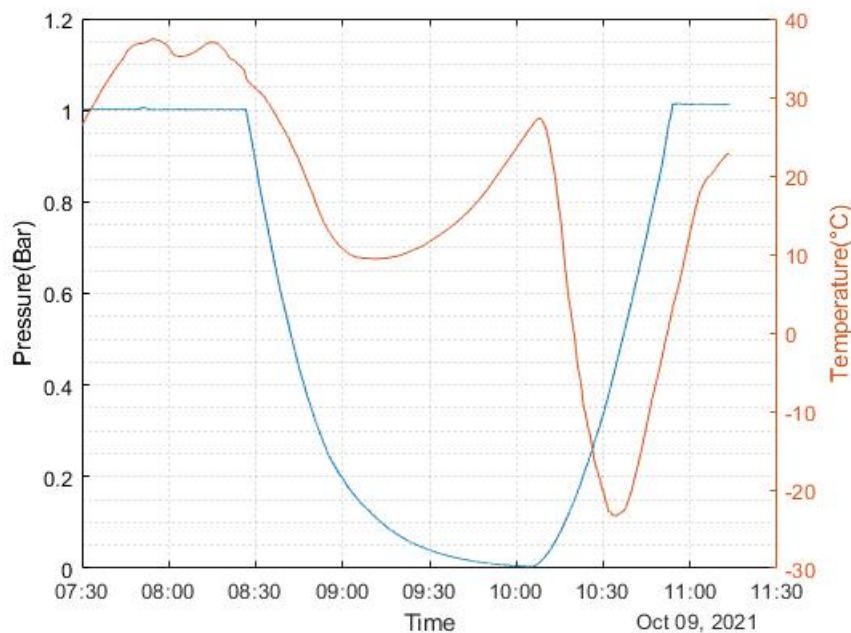


Fig. 4.1: DUM - flight test 1.

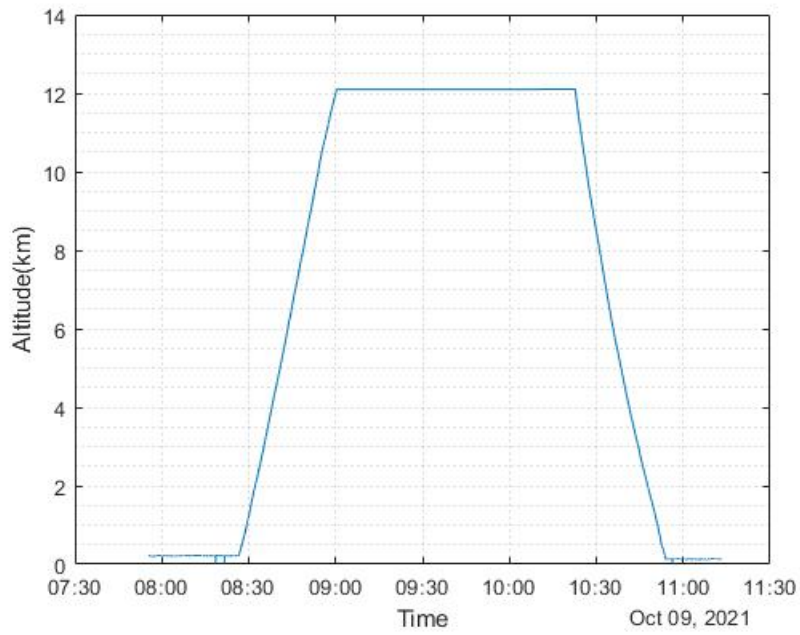


Fig. 4.2: DUM - flight test 1.

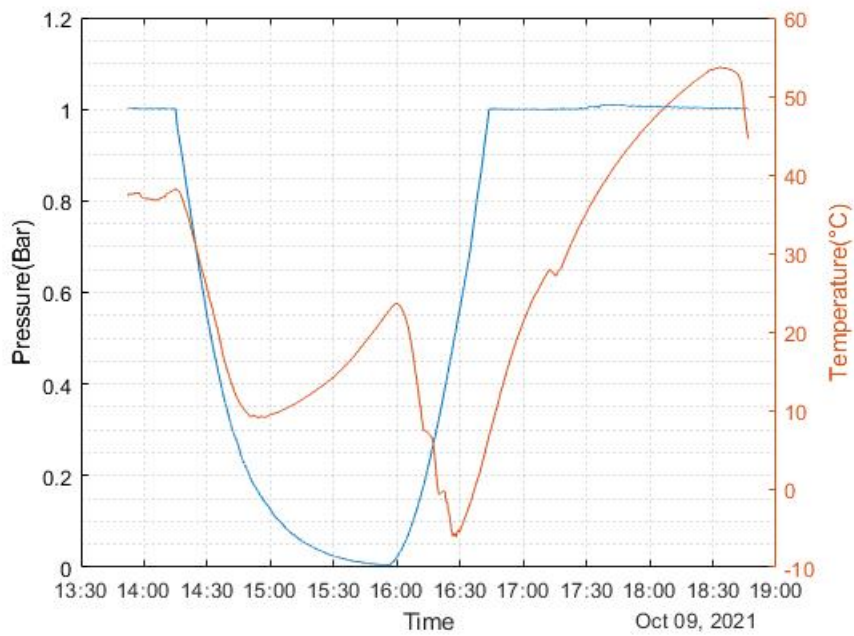


Fig. 4.3: DUM - flight test 2.

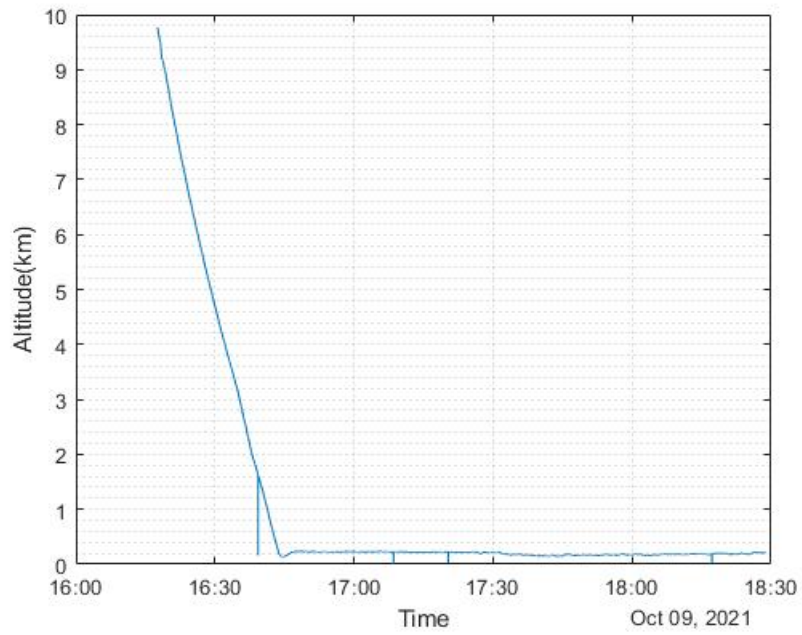


Fig. 4.4: DUM - flight test 2 altitude.

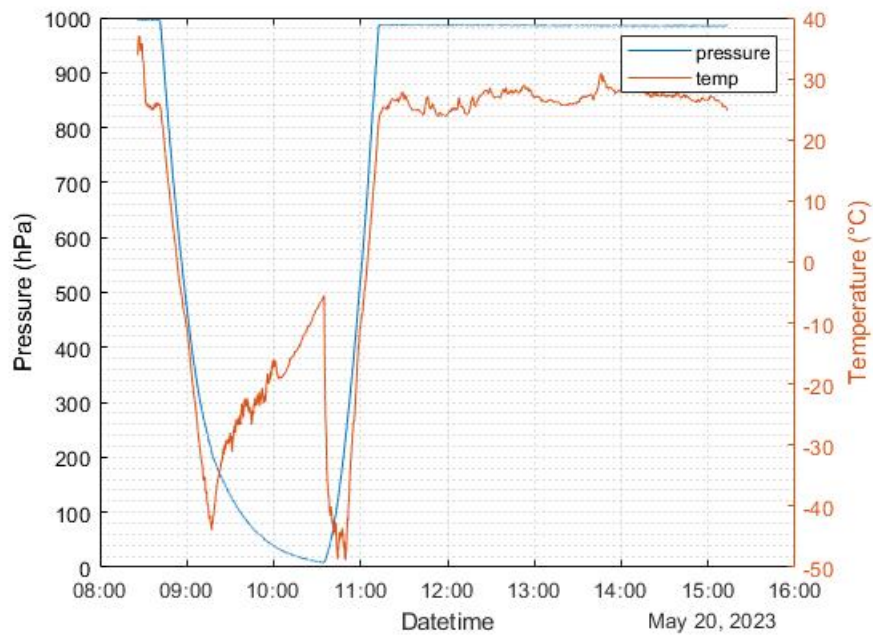


Fig. 4.5: DUM - flight test 3, Pressure.

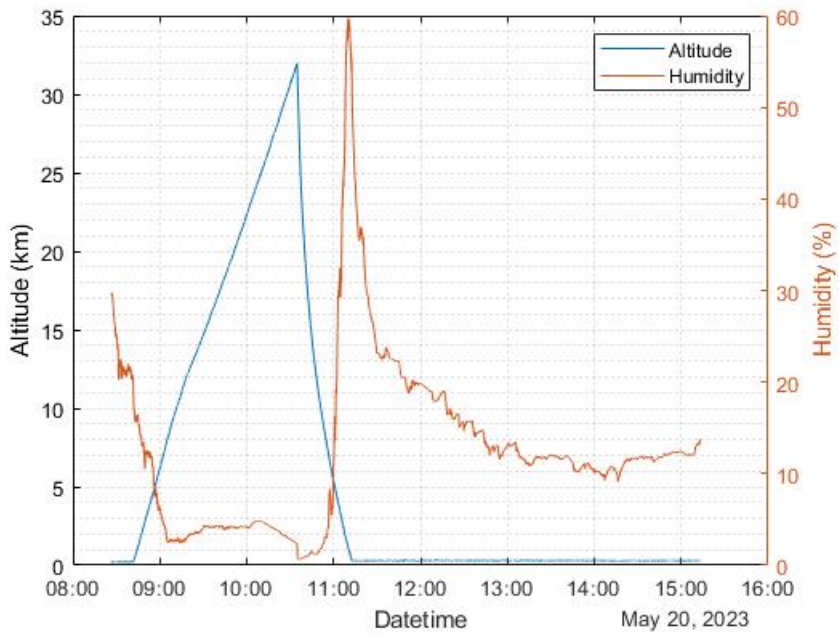


Fig. 4.6: DUM - flight test 3, Altitude.

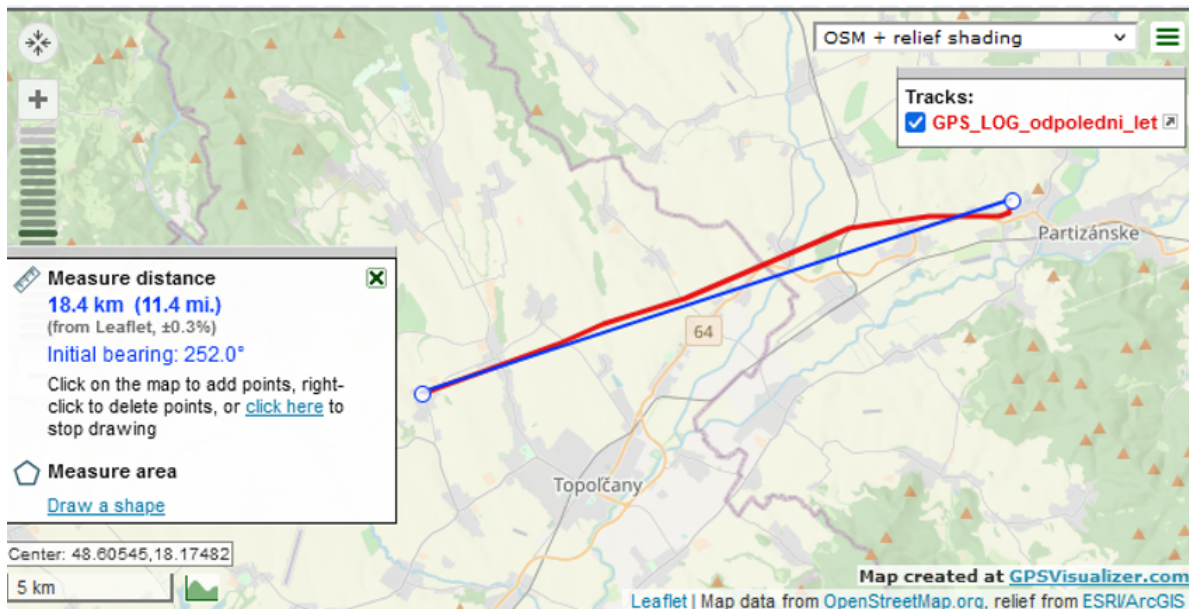


Fig. 4.7: DUM version 1

```
14:09:37.076 -> Got lora packet of type 2
14:09:37.076 -> TPS state: 0
14:09:37.076 -> Intensity 0: 0.0105698
14:09:37.076 -> Intensity 1: 0.0000186
14:09:37.076 -> Intensity 2: 0.0000365
14:09:37.076 -> Intensity 3: 0.0002859
14:09:37.117 -> with RSSI -56
14:10:07.134 -> 0.1.141.135.66.66.78.186.146.
14:10:07.134 -> Got lora packet of type 0
14:10:07.134 -> Pressure input state: 1
14:10:07.134 -> Latitude: 48.6323738
14:10:07.134 -> Longitude: 18.3409690
14:10:07.134 -> Altitude: 256.7829895
14:10:07.134 -> Speed: 2.8152000
14:10:07.134 -> with RSSI -52
14:10:37.128 -> 3.0.231.100.129.67.205.180.68
14:10:37.128 -> Got lora packet of type 3
14:10:37.128 -> TPS state: 0
14:10:37.128 -> ADC channel 0: 258.7882995
14:10:37.128 -> ADC channel 1: 49.1765632
14:10:37.128 -> ADC channel 2: 16.6759281
14:10:37.128 -> ADC channel 3: 43.6394538
14:10:37.128 -> with RSSI -50
14:11:07.142 -> 0.1.142.135.66.66.73.186.146.
14:11:07.142 -> Got lora packet of type 0
14:11:07.142 -> Pressure input state: 1
14:11:07.183 -> Latitude: 48.6323776
14:11:07.183 -> Longitude: 18.3409595
14:11:07.183 -> Altitude: 259.5209960
14:11:07.183 -> Speed: 0.3528000
14:11:07.183 -> with RSSI -51
```

Fig. 4.8: Received LoRa transmission.

5 Experimental tests

Due to the reasons from the previous chapter, the decision was taken to test the prediction of the trajectory virtually before running the prediction in a live stratospheric flight. It is done by injecting the fake ubx NAV-PVT GPS packets to the DUM and logging its overall computing variables and other peripheries, such as the pressure switch, pressure sensor, and temperature sensor. With the help of SondeHub's flight prediction software, a flight prediction of a test flight was prepared is shown in Figure 5.1, Figure 5.2 and Figure 5.3 [33].

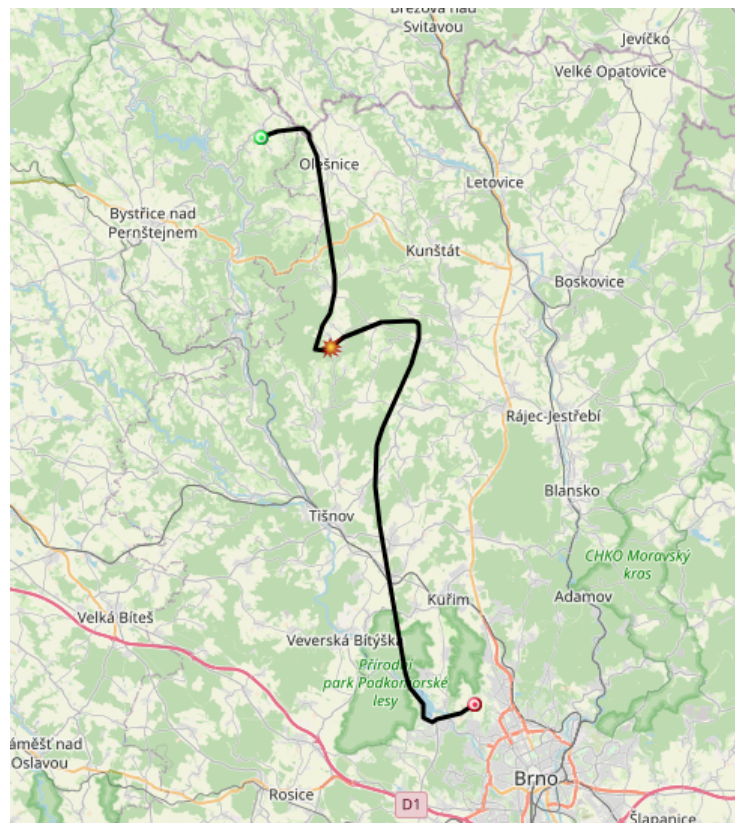


Fig. 5.1: Flight predicted by SondeHub

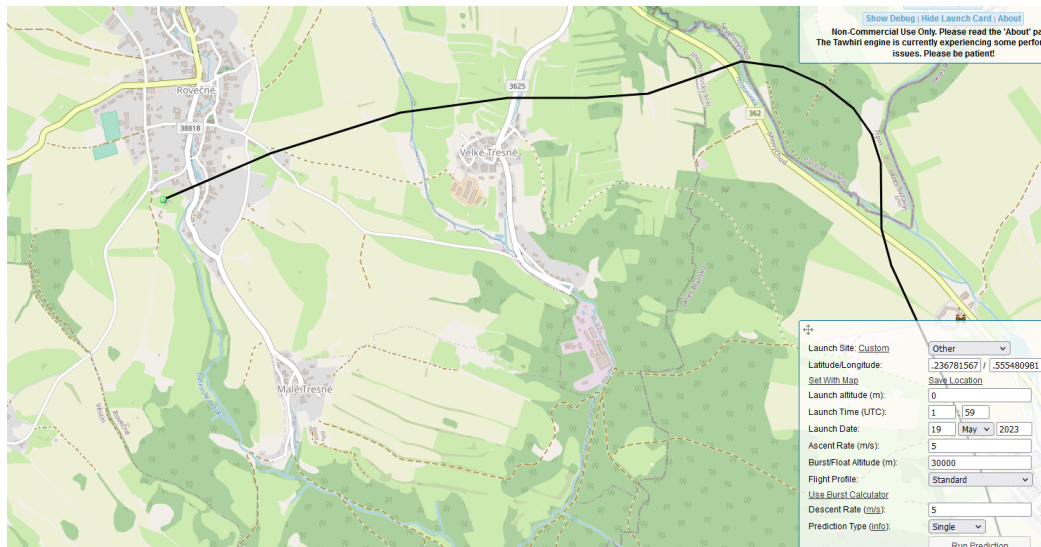


Fig. 5.2: Descending area of a flight

In the Figure 5.3, there can be seen the orange circles. That is a set dropzones that DUM should avoid. The colorful trajectory line was created and has been fed to the DUM. The start of the green color of the trajectory means the DUM computed trajectory aiming to the dropzone. Then it makes the decision to or not to release the second chute. It is done by calculating in the chute coefficient. That means the DUM will test if releasing a secondary chute of set drag coefficient or meter per second would slow down the probe enough and fly over the dropzone. In the Figure 5.4 is part of the log, when DUM has decided to release the second chute.

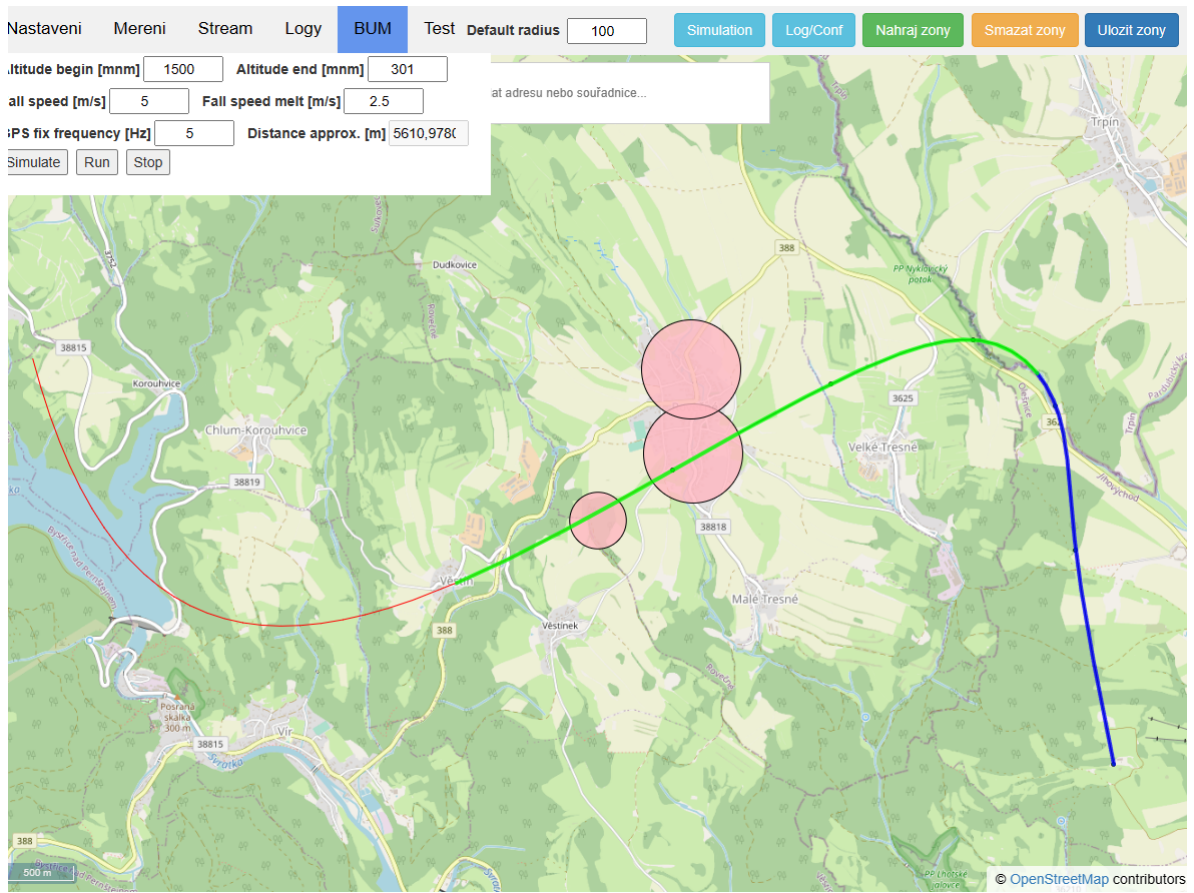


Fig. 5.3: Live virtual test

```

1
1 Drop zone hit: 16.3621883 49.5799103 297.000Zone fit: 16.3631096 49.5789070
0 Drop zone hit: 16.3621883 49.5799103 297.000Zone fit: 16.3656178 49.5796852
0
0 Slow by 25 percent will help
0 Starting melt at 16.3954716
1
1
0 Done melting chute released!
1 Drop zone hit: 16.3621883 49.5799103 297.000Zone fit: 16.3623543 49.5789833
0
0 Slow by 25 percent will help

```

Fig. 5.4: Hitted dropzone log

Conclusion

This thesis describes the author's contribution to the SnHV project of the Valašské Meziříčí and Spacemanic company in the form of the development of a supportive landing module - the DUM.

The first part of the thesis deals with the history of ballooning and early scientific experiments and contains a description of the balloons for flying into the stratosphere and their advantages and disadvantages.

The second part describes the SnHV project, its members, and its goals and shortly describes the DUM and SUPERDUM.

The third part covers the whole process of the DUM's development and its peripheries, and its indented functionality. In Chapter 3.1 is firstly set the specification of the design parameters and rules such as low Bill of Material, small dimension and weight, and durability towards the condition in the stratosphere. Then the MCU is then chosen. The communication transceiver was selected in a set band of 868 MHz, utilising the LoRa communicating. After designing the power management, the first revision was manufactured and tested its functionality. After that, the development of the peripheries were done. The signaling LEDs, Buzzer, secondary chute release mechanism and its controlling circuits and parts were selected. Designing the experimental pressure switch was done after that, utilizing the tiny water balloon and the micro switch combining them together, followed up by designing the 3D models of the pressure switch cover. Testing it in a vacuum, the dependence on the distance between the micro switch and the balloon for the wanted altitude set point was found as shown in the Figure 3.11. Once the peripheries were chosen, the DUM revision two and revision three were made. Each iteration has brought improvements over its predecessor, as shown in Tab 3.6 and Tab 3.7. Chapter 3.10 discusses how the firmware works and how the trajectory is being predicted based on extrapolating the known GPS coordinates and the coordinates of the unwanted drop zone sites. The chapter ends with a description of the ground station.

Following Chapter 4 covers the real stratospheric test and the overall performance of the DUM in such environment. Three stratospheric tests were done in total, in which the DUM was thoroughly tested.

The last Chapter 5 shows the virtual experimental test of the DUM's trajectory predicting. The "actual" virtual flight test was done with the help of the SondeHub's flight predicting app, which predicted flight trajectory was put in the test as shown in Figure 5.2 Figure 5.3.

The main output of the thesis are two fully functional universal boards, the revision two and the revision three, which have been tested in stratospheric conditions.

Bibliography

- [1] YAJIMA, Nobuyuki, Naoki IZUTSU, Takeshi IMAMURA and Toyoo ABE. 2009. *Scientific Ballooning: Technology and Applications of Exploration Balloons Floating in the Stratosphere and the Atmospheres of Other Planets* [online]. 1. Springer, New York, NY. Available at: <https://doi.org/10.1007/978-0-387-09727-5>
- [2] PFOTZER, G. 1972. History of the use of balloons in scientific experiments. *Space Science Reviews* [online]. **13**(2), 200-216. Available at: <http://link.springer.com/10.1007/BF00175313>
- [3] Ionization Chamber of Victor Hess. *Museum of Radiation and Radioactivity* [online]. Available at: <https://www.orau.org/health-physics-museum/collection/ionization-chambers/radon/hess.html>
- [4] Layers of Earth's atmosphere. *Encyclopædia Britannica* [online]. Encyclopædia Britannica. Available at: <https://www.britannica.com/facts/troposphere#/media/1/606688/99826>
- [5] PIELKE, Roger A. Atmosphere. *Encyclopedia Britannica* [online]. Available at: <https://www.britannica.com/science/atmosphere>
- [6] VON EHRENFRIED, Manfred "Dutch". 2021. *Stratospheric Balloons* [online]. 1. Cham: Springer International Publishing. Available at: <https://doi.org/10.1007/978-3-030-68130-2>
- [7] Soaring Heights. New Horizons. *Raven aerostar* [online]. Available at: <https://ravenaerostar.com/products/balloons-airships/zero-pressure-balloons>
- [8] ABDULLAH, F., M. MATSUOKA, K. OKUYAMA and A. HANAZAWA. 2018. Stratosphere Observation Project Using a Small Balloon. *Environment and Ecology Research* [online]. **6**(4), 270-283. Available at: http://www.hrpub.org/journals/article_info.php?aid=7151
- [9] OSD335x C-SiP Family. *Octavo Systems* [online]. Available at: <https://octavosystems.com/docs/osd335x-c-sip-datasheet/>
- [10] DEL CAMPO, Guillermo, Igor GOMEZ, Guillermo CAÑADA, Luca PIOVANO and Asuncion SANTAMARIA. 2020. Guidelines and criteria for selecting the optimal low-power wide-area network technology. *LPWAN Technologies for IoT and M2M Applications* [online]. Elsevier, p. 281-305. Available at: <https://linkinghub.elsevier.com/retrieve/pii/B9780128188804000144>

- [11] LIBERG, Olof, Mårten SUNDBERG, Y.-P. Eric WANG, Johan BERGMAN and Joachim SACHS. 2018. The Competitive Internet of Things Technology Landscape. *Cellular Internet of Things* [online]. Elsevier, p. 327-360. Available at: <https://linkinghub.elsevier.com/retrieve/pii/B9780128124581000095>
- [12] RP2-1.0.3 LoRaWAN® Regional Parameters. *LoRa Alliance* [online]. Available at: https://lora-alliance.org/resource_hub/rp2-1-0-3-lorawan-regional-parameters/
- [13] General Authorisation No. VO-R/10/03.2021-4 for the use of radio frequencies and for the operation of short-range devices. 2021. *Czech Telecommunication Office* [online]. Prague. Available at: https://www.ctu.eu/sites/default/files/obsah/stranky/74784/soubory/vo-r10-03.2021-4enfin_0.pdf#page=3
- [14] Všeobecné povolenie č. VPR — 01/2021. *Úrad pre reguláciu elektronických komunikácií a poštových služieb* [online]. Available at: https://www.teleoff.gov.sk/data/files/49983_vestnik1.pdf
- [15] ESP32WROOM32E Datasheet. *Espressif* [online]. Available at: https://www.espressif.com/sites/default/files/documentation/esp32-wroom-32e_esp32-wroom-32ue_datasheet_en.pdf
- [16] STM32U575xx datasheet. 2022. *STMicroelectronics* [online]. Available at: <https://www.st.com/resource/en/datasheet/stm32u575ag.pdf>
- [17] LPC55S2x/LPC552x datasheet. 2021. *NXP Semiconductor* [online]. Available at: https://www.nxp.com/docs/en/nxp/data-sheets/LPC55S2x_LPC552x_DS.pdf
- [18] Low Power Long Range Transceiver Module: Model No.:RFM95W/96W/98W. *HopeRF* [online]. Available at: <https://www.hoperf.com/data/upload/portal/20190801/RFM95W-V2.0.pdf>
- [19] Lambda62 LoRa Transceiver. *RF Solutions* [online]. Available at: <https://www.rfolutions.co.uk/downloads/6245d5b701fe6985DS-LAMBDA62-6.pdf>
- [20] MultiTech xDot: Long Range LoRa Module. *MultiTech* [online]. Available at: <https://www.multitech.com/documents/publications/data-sheets/86002182.pdf>
- [21] STUTZMAN, Warren L. and Gary A. THIELE. 2013. *Antenna theory and design*. 3rd edition. Hoboken, NJ: Wiley.

- [22] ALLAN, Alasdair. 2019. A New LoRaWAN Distance Record. *Hackster.io* [online]. Available at: <https://www.hackster.io/news/a-new-lorawan-distance-record-577c8bc11d7b>
- [23] *OVERVIEW OF LITHIUM ION BATTERIES* [online]. Available at: https://api.pim.na.industrial.panasonic.com/file_stream/main/fileversion/3455
- [24] BUCHMANN, Isidor. 2011. *Batteries in a portable world: a handbook on rechargeable batteries for non-engineers*. Cadex Electronics.
- [25] Battery Cell Comparison. *Epec Engineered Technologies* [online]. Available at: <https://www.epectec.com/batteries/cell-comparison.html>
- [26] NEO-6 u-blox 6 GPS Modules: data sheet. *U-blox* [online]. Available at: https://content.u-blox.com/sites/default/files/products/documents/NEO-M8_ProductSummary_UBX-16000345.pdf
- [27] *NCR18650GA data sheet* [online]. Available at: https://www.omnitron.cz/_dokumenty/792019123600416/ncr-18650ga.pdf
- [28] *LoRaWAN® distance world record broken, twice*. [online]. Available at: <https://www.thethingsnetwork.org/article/lorawan-distance-world-record>
- [29] *OVLEW1CB9 White High-Intensity LED Lamp datasheet* [online]. Available at: <https://cz.mouser.com/datasheet/2/414/OVLEW1CB9-3011953.pdf>
- [30] Webench power designer. *Texas Instruments* [online]. Available at: <https://webench.ti.com/power-designer/>
- [31] EASTER-ROBINSON, Rowan. *ArduinoCurveFitting*. [Https://github.com/Rotario/arduinoCurveFitting](https://github.com/Rotario/arduinoCurveFitting) [online]. Available at: <https://github.com/Rotario/arduinoCurveFitting>
- [32] *Dragino LoRa Shield* [online]. Available at: https://wiki1.dragino.com/index.php/Lora_Shield
- [33] *SondeHub amateur* [online]. Available at: <https://amateur.sondehub.org/>
- [34] *SC4617EBHZGTLR transistor datasheet* [online]. Available at: https://cz.mouser.com/datasheet/2/348/rohm_s_a0008265177_1-2281854.pdf
- [35] *FZT651QT transistor datasheet* [online]. Available at: https://cz.mouser.com/datasheet/2/115/DIOD_S_A0000570260_1-2541856.pdf

Symbols and abbreviations

ADC	Analog to digital converter
BJP	Bipolar Junction Transistor
C-Sip	Complete System in Package
DC	Direct Current
DIY	Do It Yourself
FSPL	Free Space Path Loss
GPS	Global Positioning System
GPIO	General Purpose Input Output
GS	Ground Station
HAB	High Altitude Balloon
ISM	Industrial Scientific Medical
LDO	Low Drop Out regulator
LoS	Line of Sight
LPWAN	Low Power Wide Area Network
MCU	Micro Controller unit
OBC	Onboard Computer
PWM	Pulse Width Modulation
SoC	System on Chip
SOSA	Slovak Organization for Space Activities
LDB	Long Duration Balloon
SPB	Super Pressure Balloon
UART	Universal Asynchronous Receiver Transmitter
ZPB	Zero Pressure Balloon

List of appendices

A Schematics	77
A.1 DUM revision 1	77
A.2 DUM revision 2	77
A.3 DUM revision 3	77
A.4 DUM - firmware flowchart	77
B Electronic Attachment Table of Contents	91

A Schematics

A.1 DUM revision 1

A.2 DUM revision 2

A.3 DUM revision 3

A.4 DUM - firmware flowchart

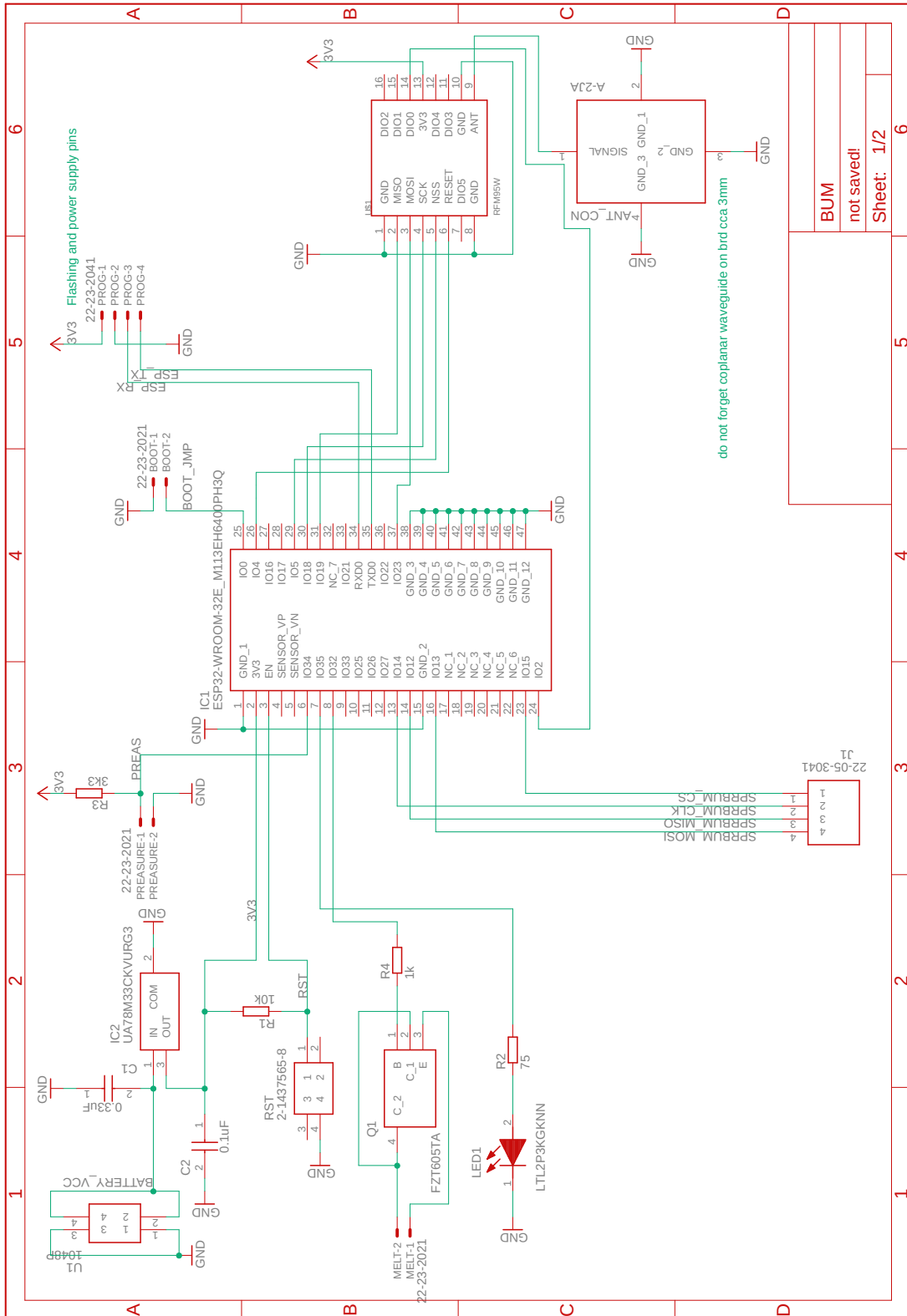


Fig. A.1: DUM revision 1 schematic

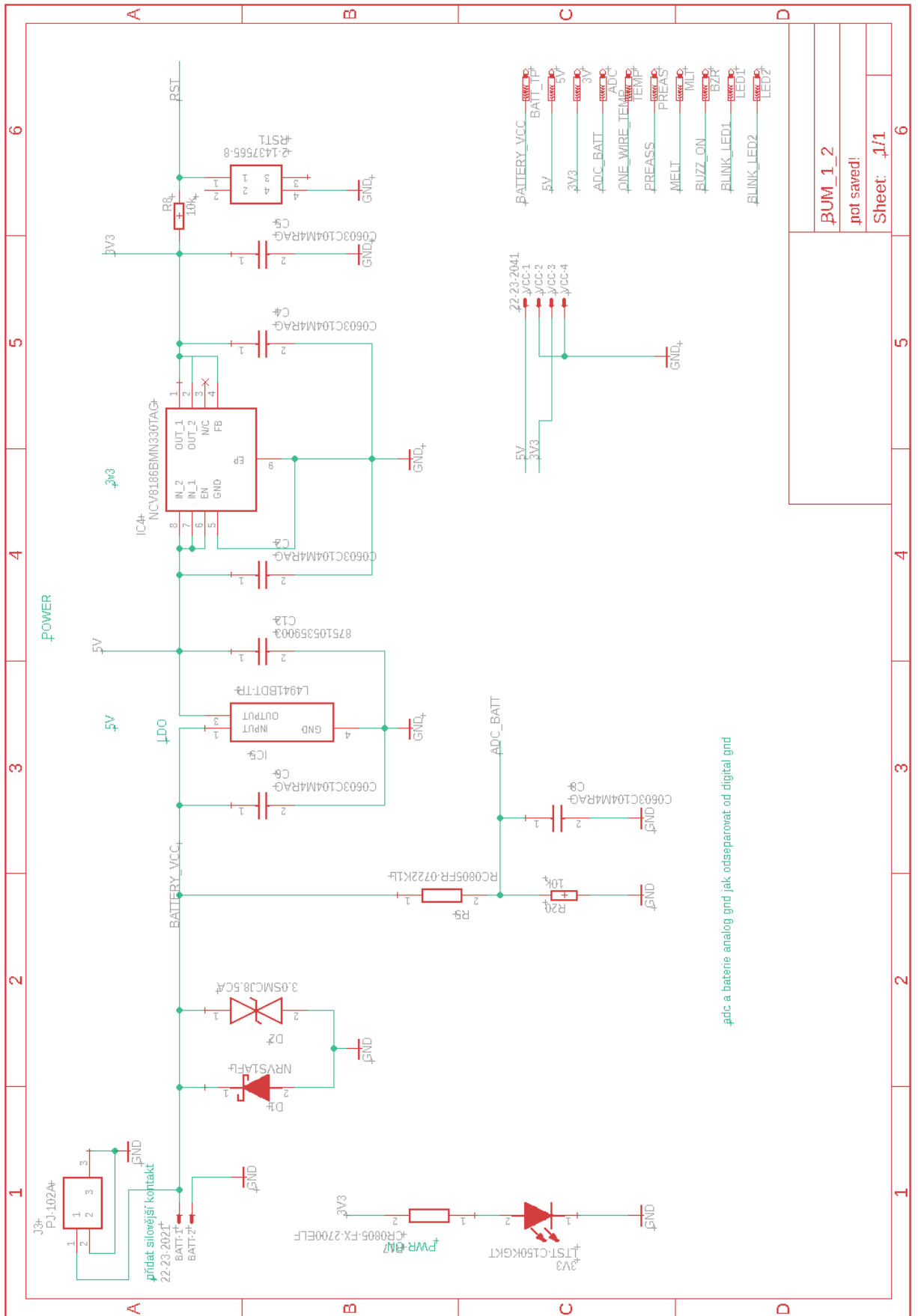
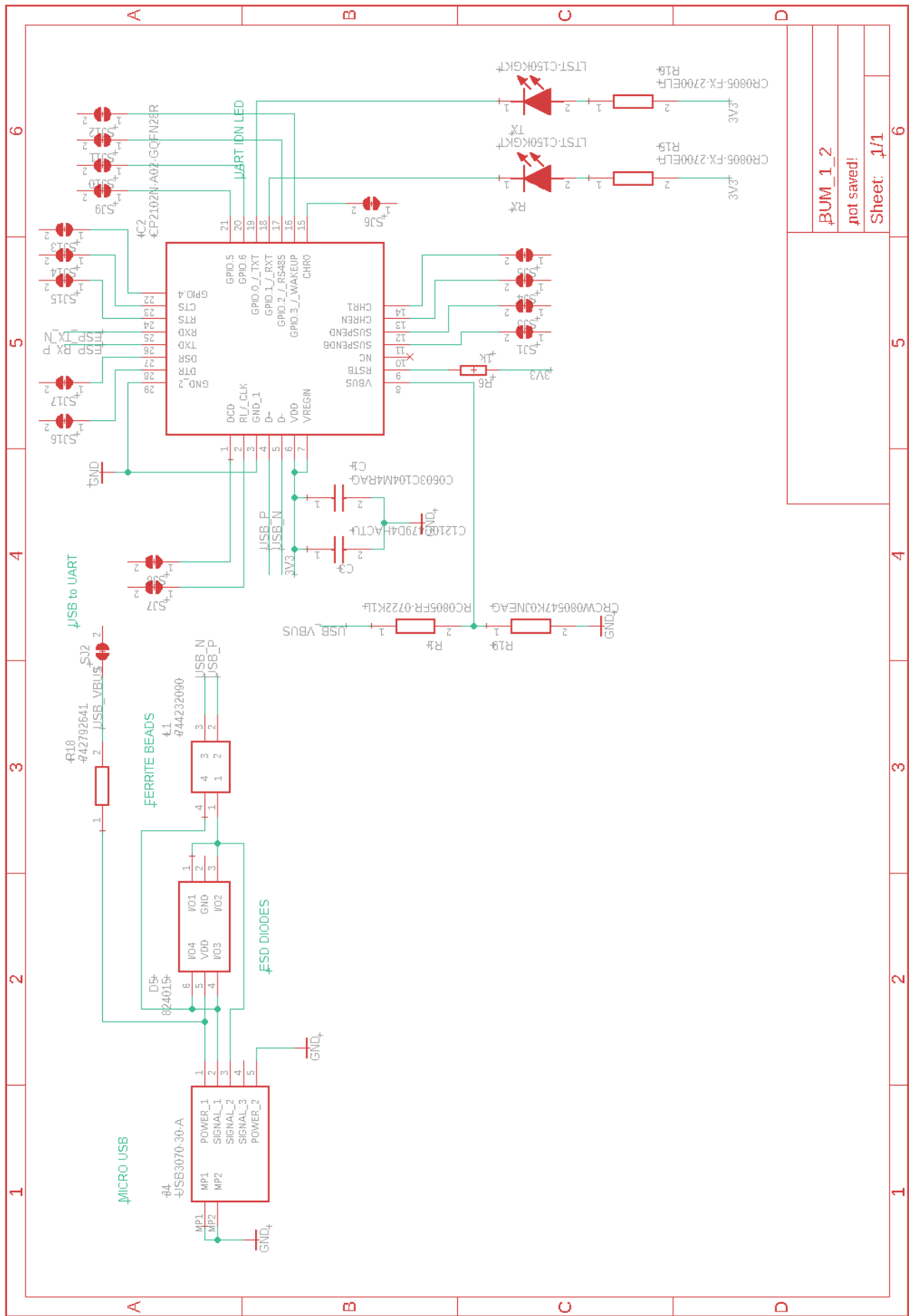


Fig. A.2: DUM revision 2 schematic (Page 1/4)

BUM_1_2		6	
not saved!		5	
Sheet: 1/1		4	
		3	
		2	
		1	



BUM_1_2
.not saved!
Sheet: 1/1

Fig. A.3: DUM revision 2 schematic (Page 2/4)

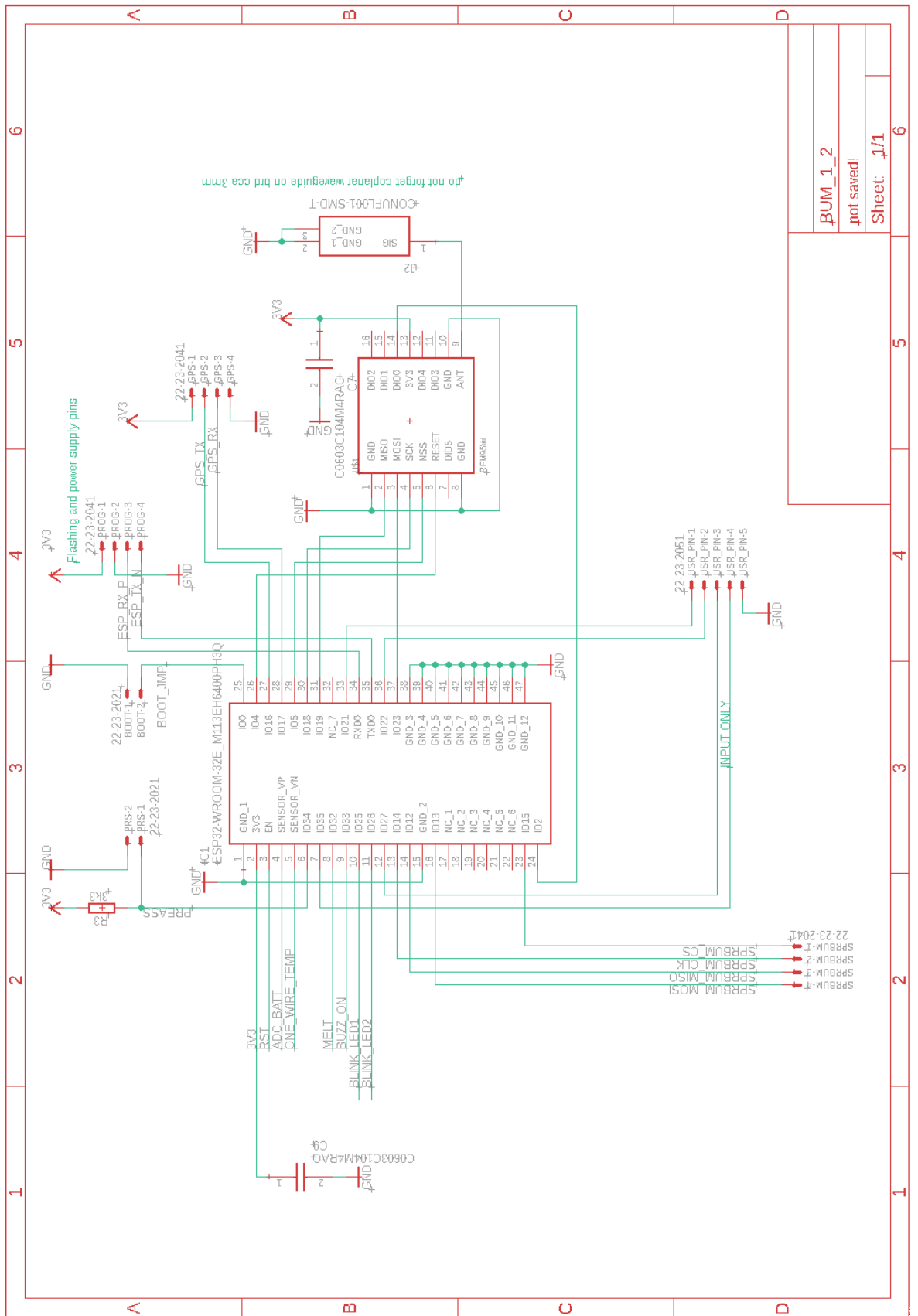


Fig. A.4: DUM revision 2 schematic (Page 3/4)

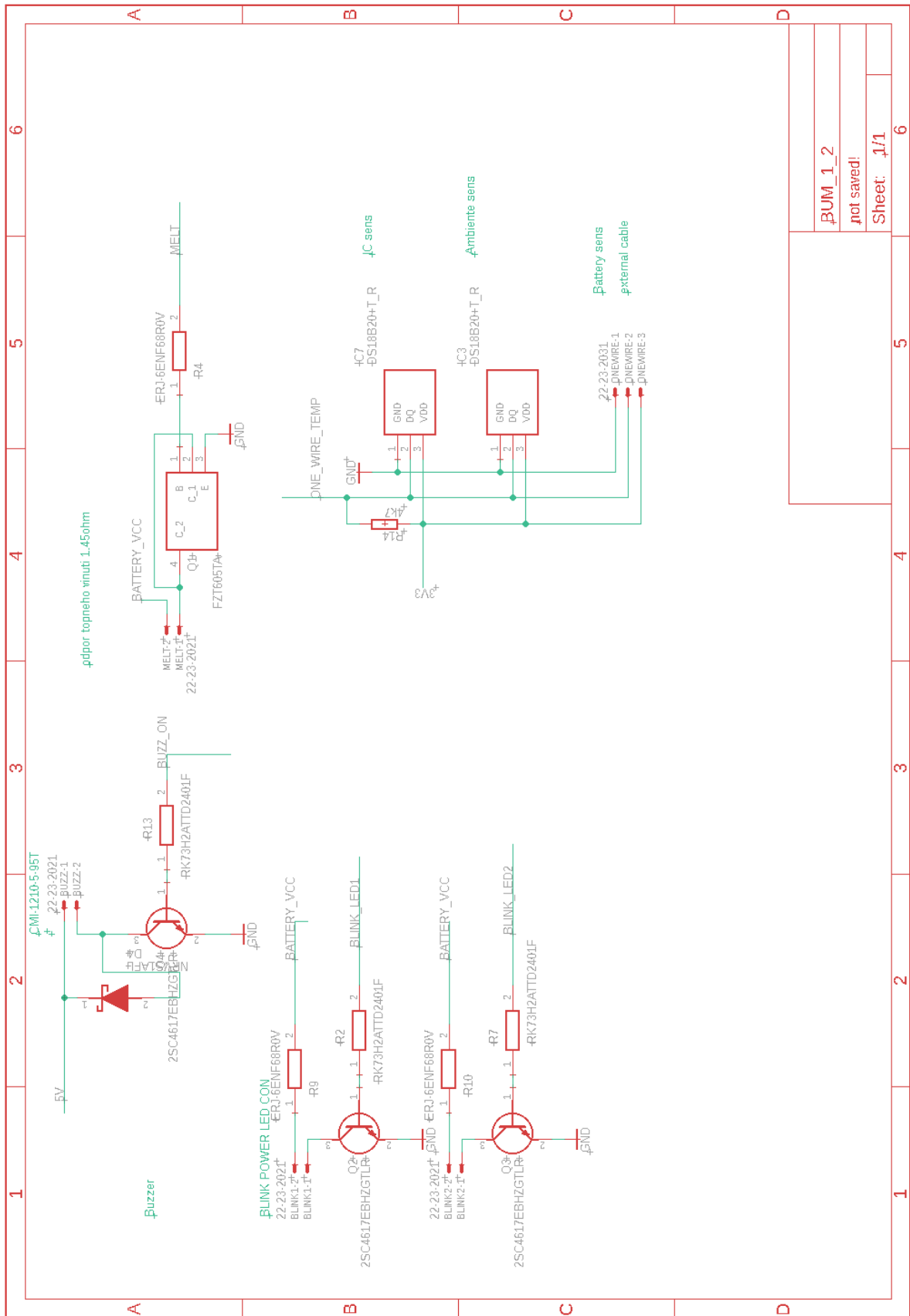


Fig. A.5: DUM revision 2 schematic (Page 4/4)

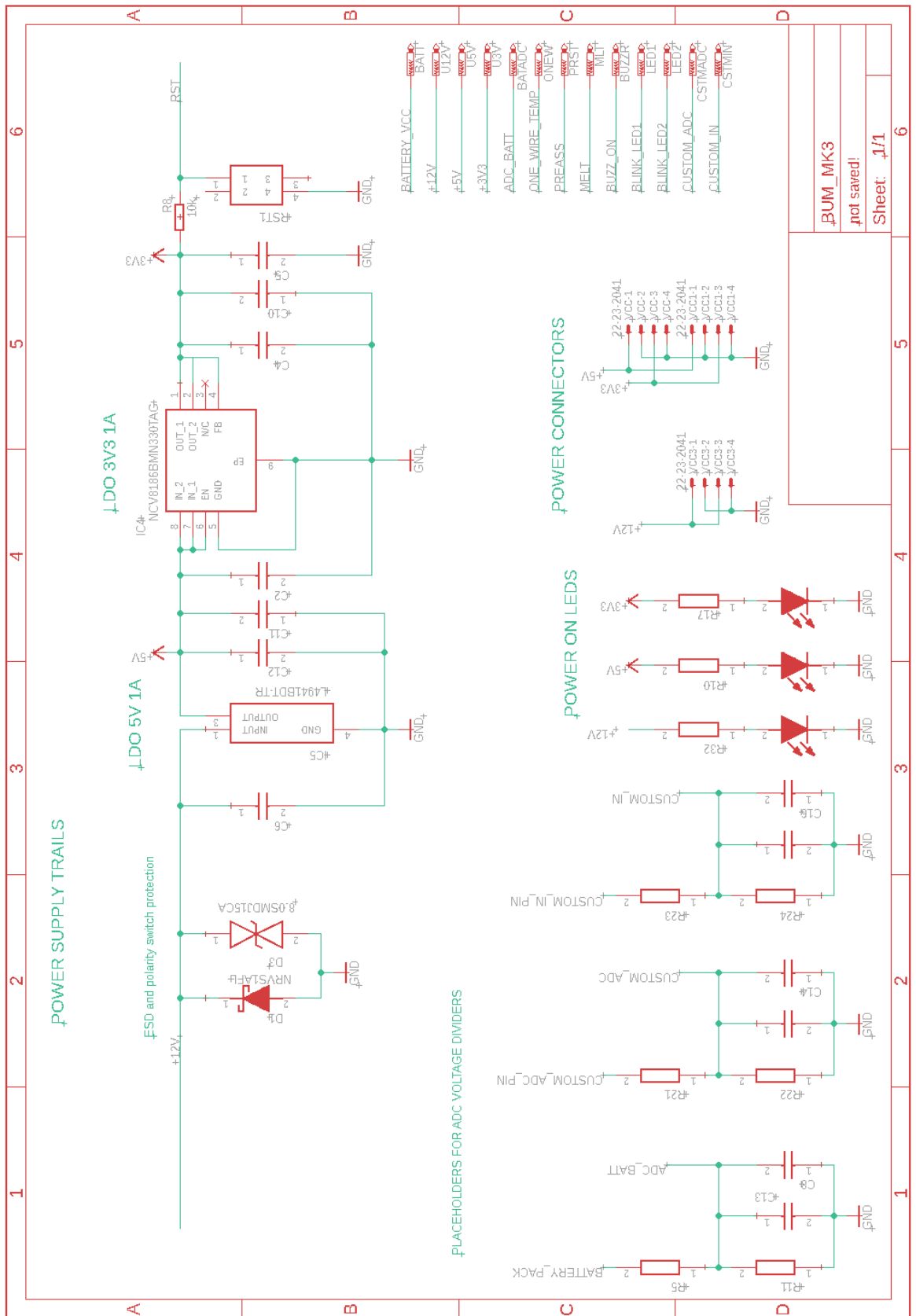


Fig. A.6: DUM revision 3 schematic (Page 1/6)

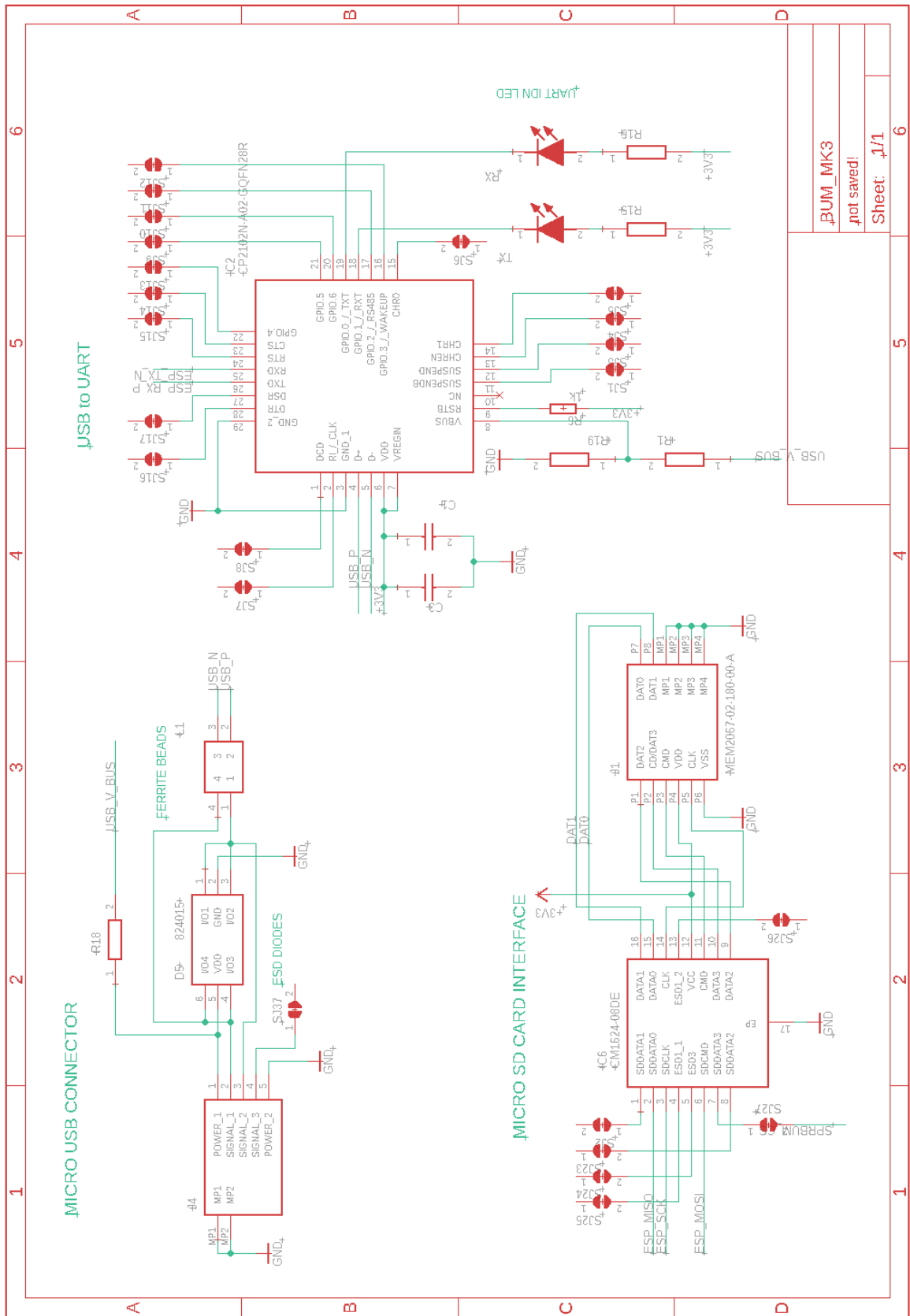


Fig. A.7: DUM revision 3 schematic (Page 2/6)

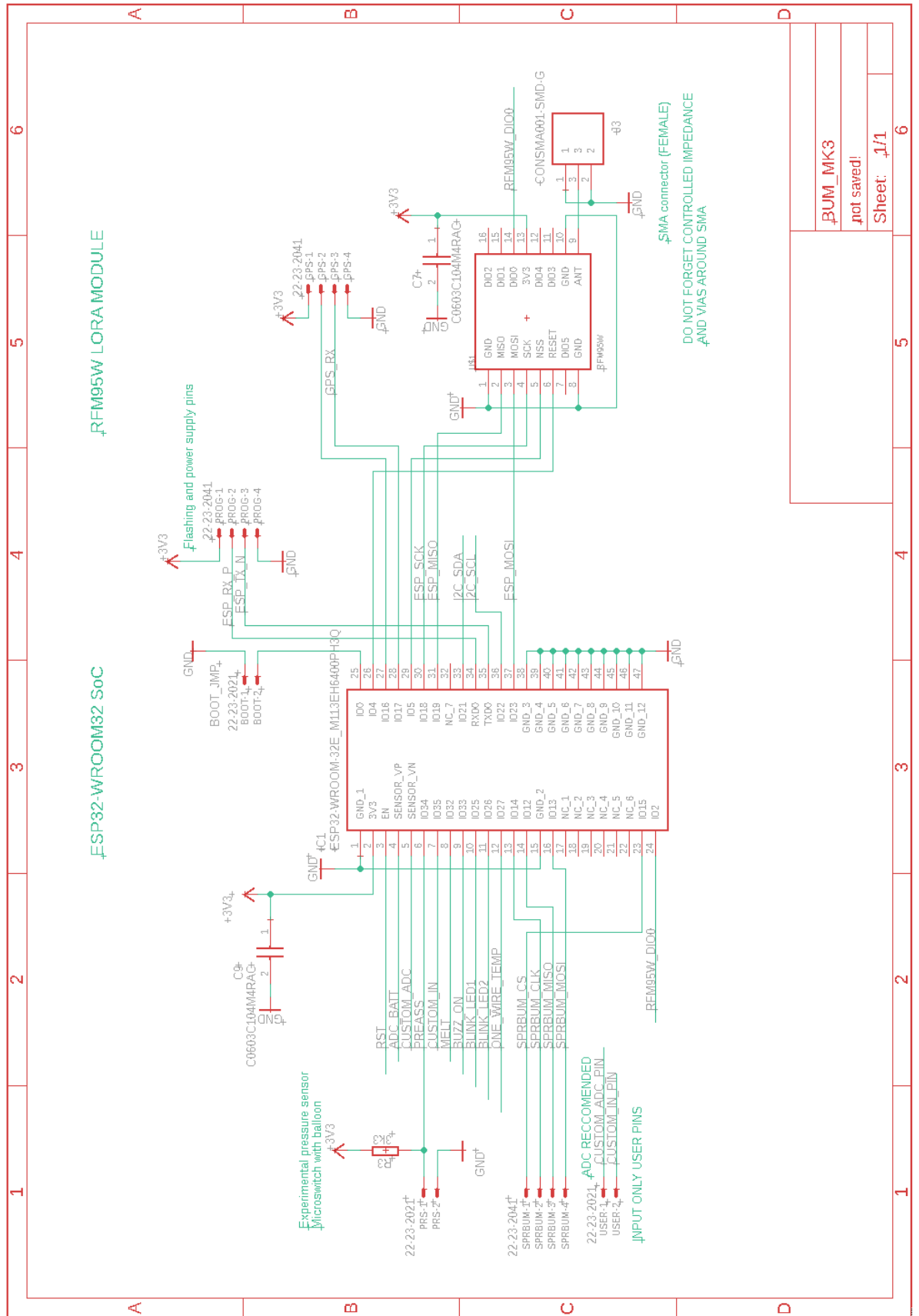


Fig. A.8: DUM revision 3 schematic (Page 3/6)

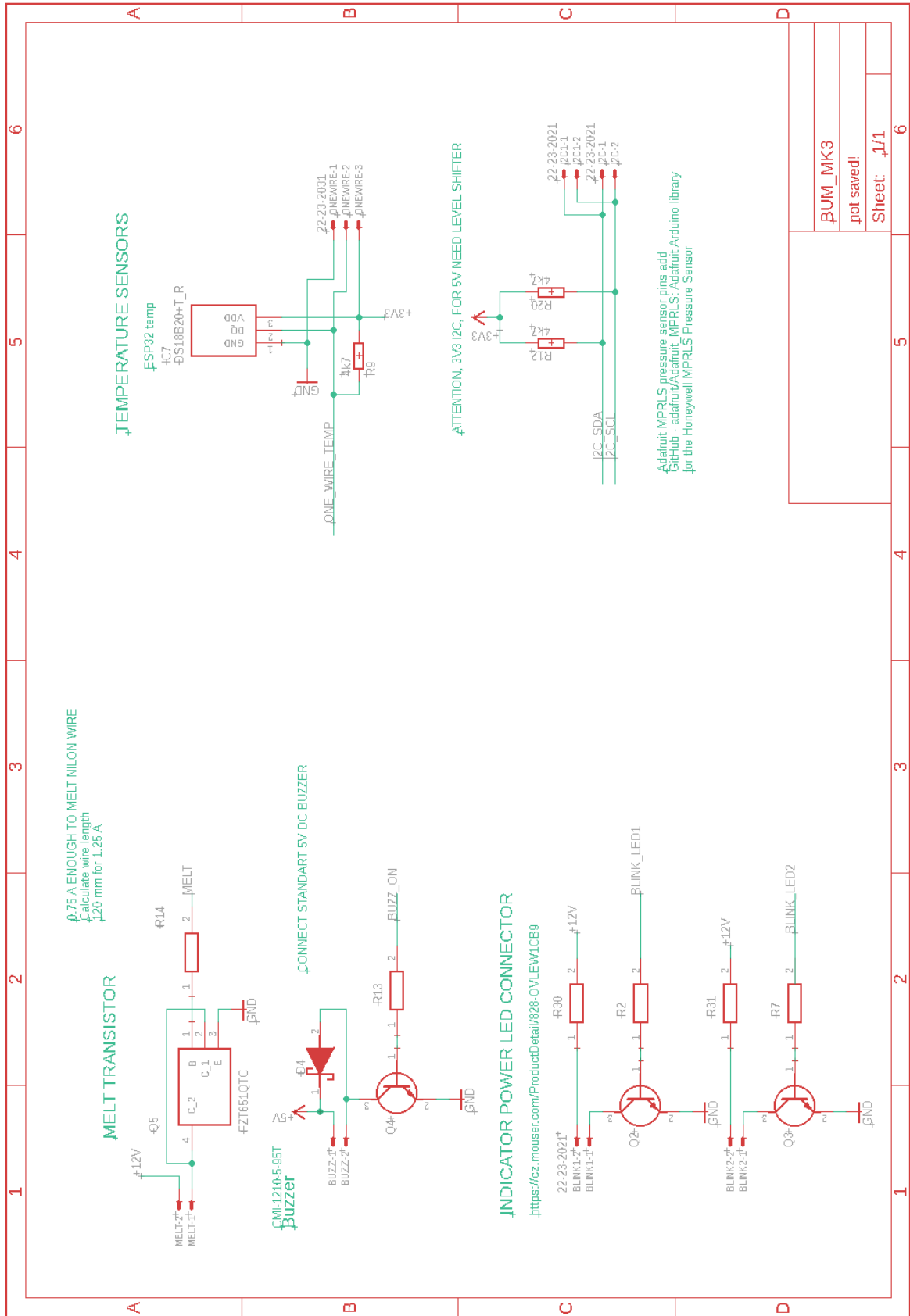


Fig. A.9: DUM revision 3 schematic (Page 4/6)

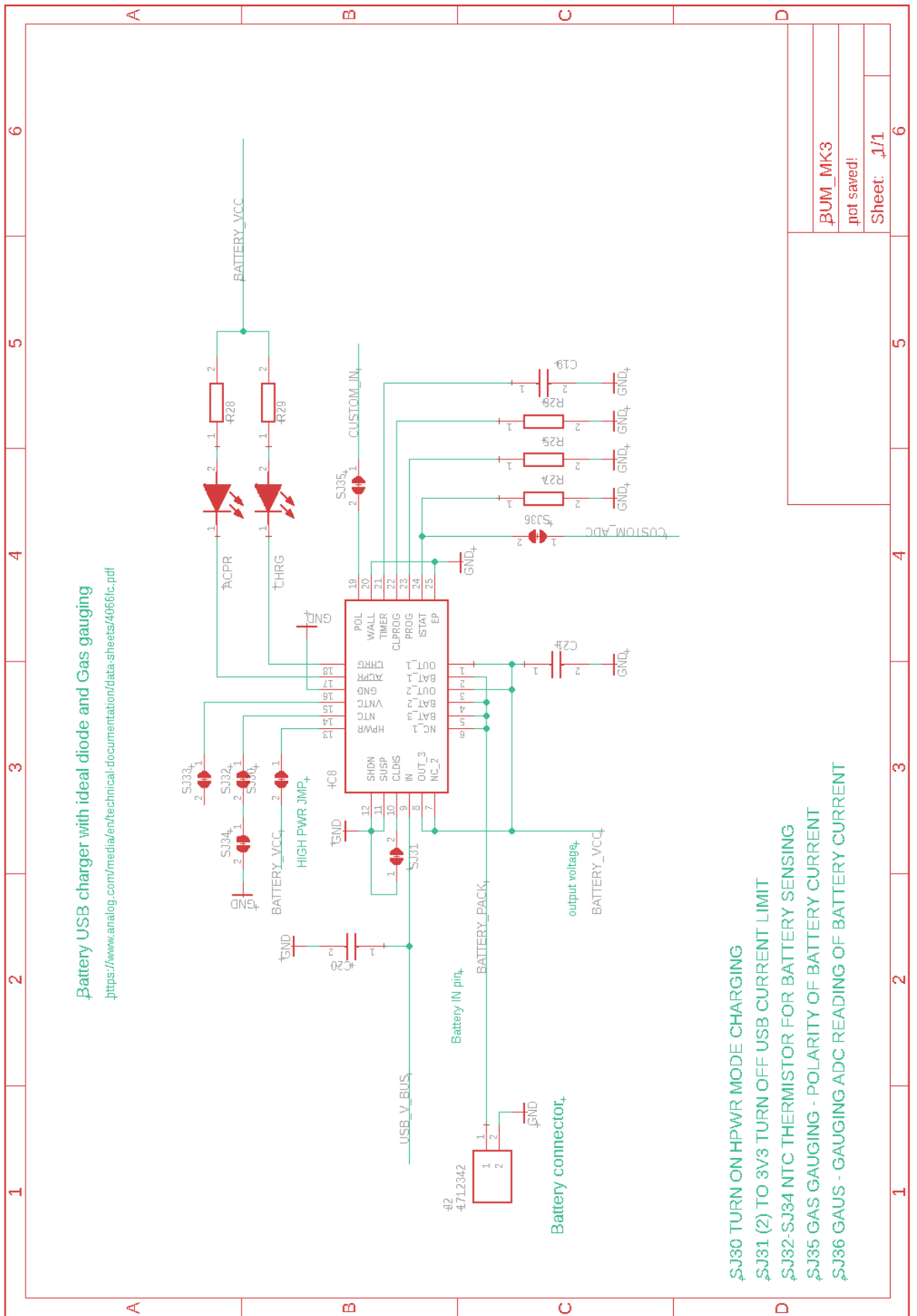
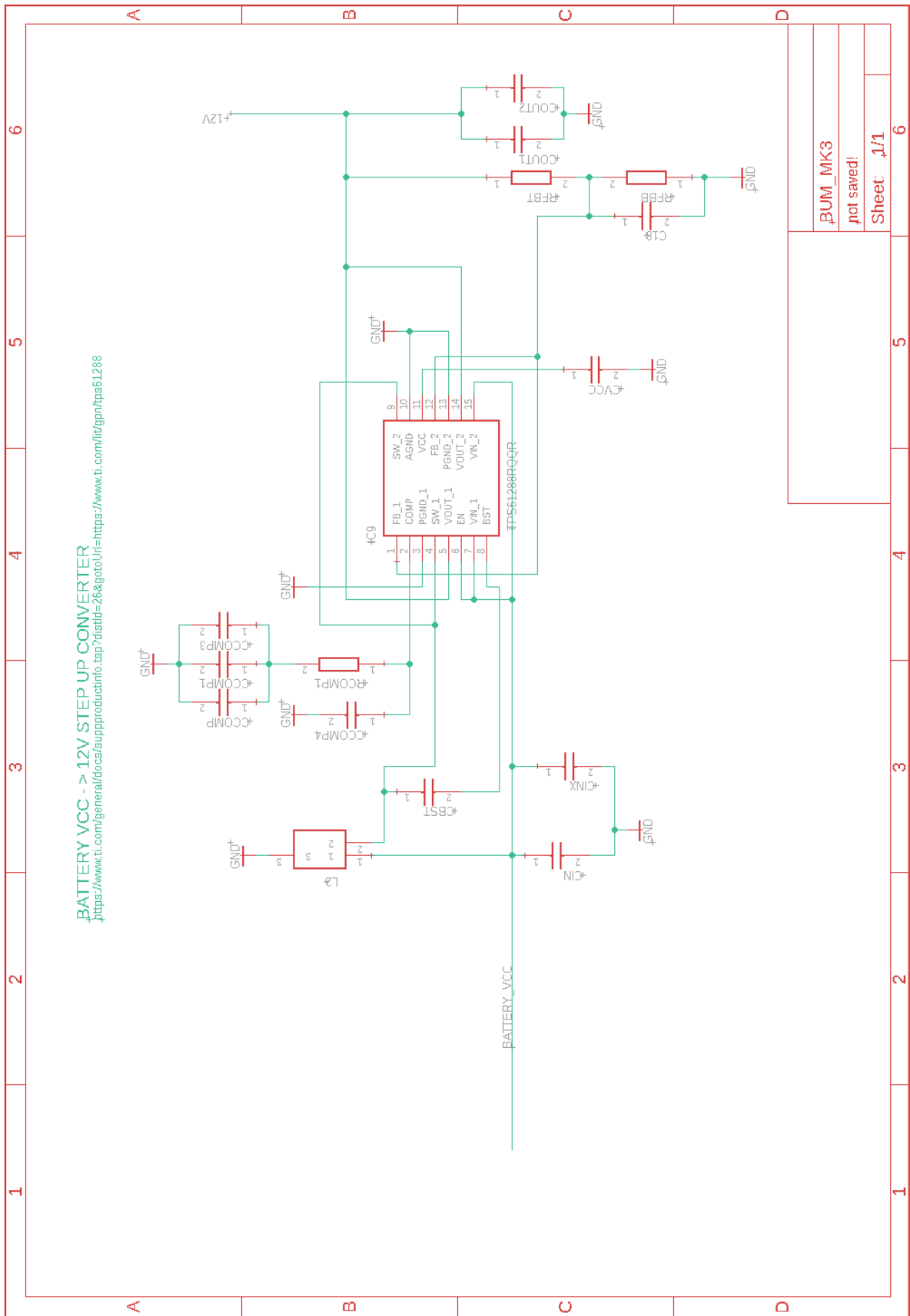


Fig. A.10: DUM revision 3 schematic (Page 5/6)



BUM_MK3	
not saved!	
Sheet: 1/1	6

Fig. A.11: DUM revision 3 schematic (Page 6/6)

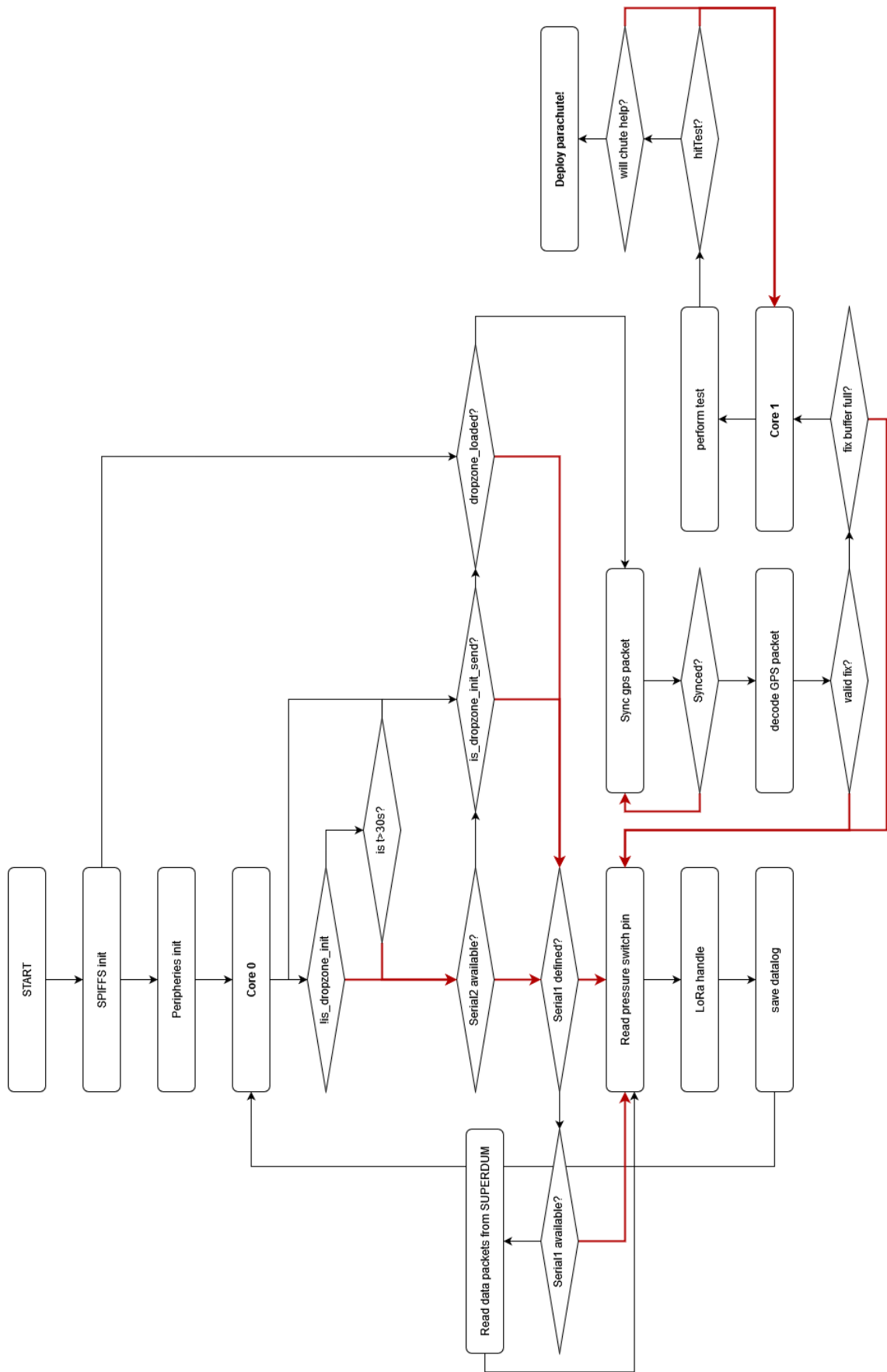


Fig. A.12: DUM firmware flowchart

B Electronic Attachment Table of Contents

/	root
├	3D models.....	Pressure switch 3D models
│	├	Ependorf_bottom_holder.SLDPRT
│	├	Ependorf_bottom_holder.STL
│	├	Ependorf_top_holder.SLDPRT
│	├	Ependorf_top_holder.STL
├	PCB.....	Schematics, layouts, BOM
│	├	MK1
│	├	MK2
│	├	MK3
├	SW.....	Firmware files
│	├	DUM.rar
│	├	LORA_receiver.rar